



THE CUSP–HOPF BIFURCATION*

J. HARLIM

*Courant Institute of Mathematical Sciences, New York University,
251 Mercer Street, New York, NY10012-1185, USA
jharlim@courant.nyu.edu*

W. F. LANGFORD

*Department of Mathematics and Statistics, University of Guelph,
Guelph ON, N1G 2W1 Canada
wlangfor@uoguelph.ca*

Received March 1, 2006; Revised June 28, 2006

The coalescence of a Hopf bifurcation with a codimension-two cusp bifurcation of equilibrium points yields a codimension-three bifurcation with rich dynamic behavior. This paper presents a comprehensive study of this *cusp–Hopf bifurcation* on the three-dimensional center manifold. It is based on truncated normal form equations, which have a phase-shift symmetry yielding a further reduction to a planar system. Bifurcation varieties and phase portraits are presented. The phenomena include all four cases that occur in the codimension-two fold–Hopf bifurcation, in addition to bistability involving equilibria, limit cycles or invariant tori, and a fold–heteroclinic bifurcation that leads to bursting oscillations. Uniqueness of the torus family is established locally. Numerical simulations confirm the prediction from the bifurcation analysis of bursting oscillations that are similar in appearance to those that occur in the electrical behavior of neurons and other physical systems.

Keywords: Hopf bifurcation; cusp; codimension-three; bistability; bursting oscillations.

1. Introduction

More than a quarter-century ago, it was found that the interaction of a steady-state bifurcation (corresponding to a simple zero eigenvalue) with a Hopf bifurcation (corresponding to a conjugate pair of simple imaginary eigenvalues) can lead to much richer dynamics than just the expected equilibrium and periodic solutions, including the possibility of an invariant two-torus on which the flow may be periodic or quasi-periodic, see [Gavrilo, 1978; Langford, 1979; Guckenheimer, 1980; Iooss & Langford, 1980]. As this two-torus grows fatter, generic perturbations lead to chaotic dynamics [Holmes, 1980; Langford, 1982, 1983, 1984b]. The simplest case is the codimension-two *fold–Hopf bifurcation*,

for which the zero eigenvalue corresponds to a generic fold (or saddlenode) bifurcation in which two equilibria coalesce and disappear. That case is described in textbooks such as [Guckenheimer & Holmes, 1986; Wiggins, 1990; Chow *et al.*, 1994; Kuznetsov, 2004]. This paper presents a study of a more degenerate case, which we call the *cusp–Hopf bifurcation*, in which the fold bifurcation is replaced by a codimension-two cusp bifurcation; that is, the zero eigenvalue remains simple, but the leading quadratic term that normally determines the fold bifurcation is now assumed to be zero while a critical cubic term is nonzero. This case is said to have codimension three and has also been called a hysteresis–Hopf bifurcation.

*This work was supported in part by the Natural Sciences and Engineering Research Council of Canada.

It was first studied in [Gavrilov & Roschin, 1983; Langford, 1983, 1984a, 1984b; Gavrilov, 1987].

Specifically, we consider a parameterized family of ordinary differential equations

$$\dot{x} = f(x, \mu), \quad x \in \mathbb{R}^n, \quad \mu \in \mathbb{R}^p, \quad (1)$$

where f is smooth with respect to x and μ , $\dot{x} \equiv dx/dt$, and μ represents parameters in the equation. Let $x = x_0$ be an equilibrium point of the system for $\mu = \mu_0$, i.e. $f(x_0, \mu_0) = 0$. For each μ the solutions of (1) define a flow of a dynamical system, at least locally in t .

The ultimate goal of this research is a complete description of the dynamics of system (1) near a cusp–Hopf bifurcation, analogous to what has been achieved for the fold–Hopf case. This paper presents significant new understanding of the cusp–Hopf bifurcation, which has richer possibilities than the fold–Hopf case, and also brings together previous results that were incomplete and scattered in the literature. The main results are summarized in Figs. 2–4, 9, 10, 12 and 13.

1.1. The cusp manifold of equilibrium points

The simplest degenerate case of the fold bifurcation is the *cusp bifurcation* (related to the “cusp catastrophe” of Catastrophe Theory, see [Thom, 1975]). This is also called a hysteresis bifurcation in [Langford, 1984a, 1984b; Golubitsky & Schaeffer, 1985]. It may occur in its simplest form with a one-dimensional state space ($n = 1$) and a two-dimensional parameter space ($p = 2$) in (1). A simple model differential equation for the cusp bifurcation is

$$\dot{z} = \beta + \alpha z - z^3, \quad (2)$$

where $z \in \mathbb{R}$ is the state variable and α and β are two bifurcation parameters (or “control” or “unfolding” parameters). This differential equation has equilibrium points lying on a two-dimensional manifold M in $\mathbb{R} \times \mathbb{R}^2$ given by

$$M = \{(z, \alpha, \beta) | \beta + \alpha z - z^3 = 0\}, \quad (3)$$

see Fig. 1. We call this manifold M the *cusp manifold*.

The projection of the cusp manifold onto the (α, β) plane yields the *cusp bifurcation variety*, consisting of two algebraic curves in the parameter plane, meeting tangentially at the cusp point $(0, 0)$,

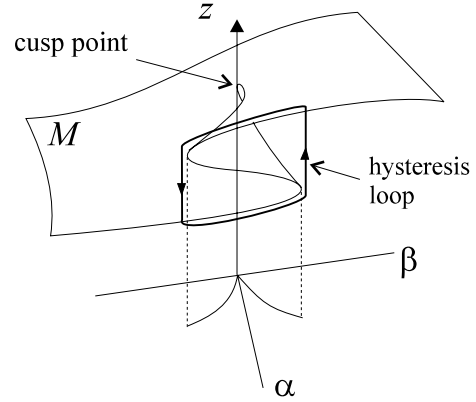


Fig. 1. The cusp manifold $M = \{\beta + \alpha z - z^3 = 0\}$ and a hysteresis loop.

as shown in Fig. 1. The equation of this cusp bifurcation variety is

$$\left(\frac{\beta}{2}\right)^2 = \left(\frac{\alpha}{3}\right)^3, \quad (4)$$

obtained by eliminating z from Eq. (3) and the equation for double roots of (3), namely $\alpha - 3z^2 = 0$. For (α, β) in the interior of the wedge bounded by the cusp bifurcation variety, there exist three distinct equilibrium points z , while exterior to this wedge there is a unique equilibrium point z . On crossing the bifurcation variety, from the interior to the exterior at any point other than the cusp point $(0, 0)$, two equilibrium points z coalesce and disappear in a fold bifurcation. Inside the wedge, the upper and lower equilibrium points z of Eq. (2) are stable, while the third equilibrium point lying between them is unstable. This coexistence of two distinct attractors at the same parameter value is called *bistability*. If β is varied with fixed $\alpha > 0$, the system jumps from one stable equilibrium to the other stable equilibrium at the two endpoints of an interval, thus tracing a *hysteresis loop* as in Fig. 1. As we increase or decrease α , the length of this hysteresis interval increases or decreases respectively, and it vanishes at the cusp point $(0, 0)$; see Fig. 1.

It may appear that Eq. (2) is a very special choice; however, it is in fact a *normal form* for a large class of differential equations which exhibit the cusp bifurcation. Suppose that the vector differential Eq. (1) has an equilibrium point with a simple zero eigenvalue and no others with zero real part; then we can perform a center manifold reduction and replace (1) with a one-dimensional equation on the center manifold ($n = 1$). This equation has an equilibrium point (which we translate to

the origin in x and μ) where $f(0,0) = 0$, and at this equilibrium point it has a zero eigenvalue, thus $f_x(0,0) = 0$. Assume that the quadratic term in the Taylor series is also zero, i.e. $f_{xx}(0,0) = 0$; but the cubic term is nonzero, i.e. $f_{xxx}(0,0) \neq 0$. Then, for generic smooth dependence on the parameters $\mu \in \mathbb{R}^2$ near 0, there are two possibilities: the equation on the center manifold is topologically equivalent, in a neighborhood of $(x, \mu) = (0,0)$, either to Eq. (2) or to the equation with $-z^3$ replaced by $+z^3$ in (2). A proof is given for example in [Kuznetsov, 2004, Chap. 8].

1.2. The cusp–Hopf bifurcation

The focus of this paper is the determination of the typical dynamical behavior when a Hopf bifurcation occurs at an equilibrium point near the cusp point, on a cusp manifold such as in Fig. 1. The limiting case of a Hopf bifurcation precisely at the cusp point is a degenerate case, which we refer to as the *cusp–Hopf bifurcation*. It is known that the existence of a Hopf bifurcation does not affect the existence of the equilibrium states on the cusp manifold (although the stabilities are affected). However, the presence of a zero eigenvalue does violate the conditions of the classical Hopf bifurcation theorem. This fact, plus the higher codimension and the fact that the state space on the center manifold has dimension three, open up possibilities for new dynamic behavior, much richer than is possible for the cusp or Hopf bifurcations separately.

Also, compared to the fold–Hopf bifurcation (as described in [Chow *et al.*, 1994; Guckenheimer & Holmes, 1986; Kuznetsov, 2004; Wiggins, 1990]), the cusp–Hopf bifurcation has richer behavior. There is the possibility of *bistability*, which is the coexistence of two different stable attractors. The two attractors may be both equilibria (as for the cusp in Fig. 1), or one may be an equilibrium point while the second is a limit cycle, invariant torus, or a chaotic attractor. Another interesting phenomenon is the occurrence of *bursting oscillations*, observed by Langford [1983], that resemble those in neurons described by Izhikevich [2000]; Rinzel [1987], or in the chemical experiments of Roux [1985], and the Taylor–Couette experiment, see [Mullin, 1993].

A further important distinction between the cusp–Hopf and fold–Hopf bifurcations is that in the cusp–Hopf case, the singular equilibrium at the codimension-three point may be asymptotically

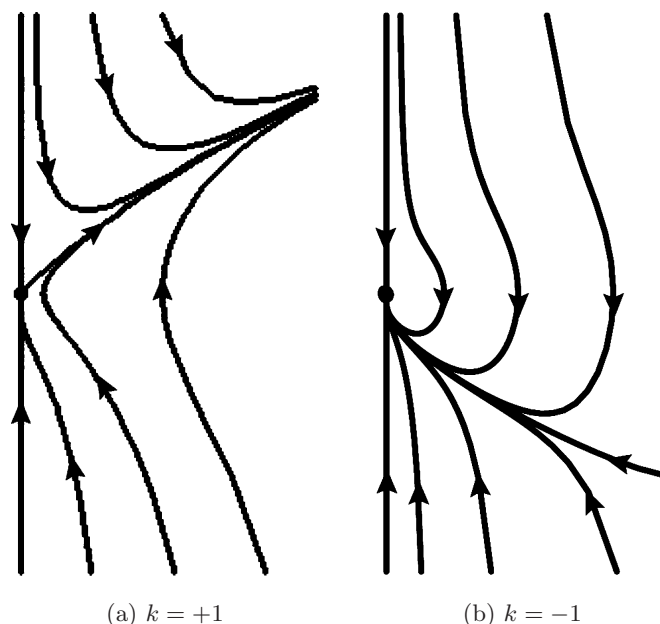


Fig. 2. Singular vector field phase portraits. ($l = -1$, $m = +1$).

stable [see Fig. 2(b)], whereas for the fold–Hopf bifurcation there is always at least one unstable direction. This fact has been observed in [Gavrilov & Roschin, 1983; Gavrilov, 1987; Langford, 1983, 1984a, 1984b]. Therefore in this case, even after unfolding, there is a basin of attraction for the local dynamics of the normal form. By contrast, in the fold–Hopf bifurcation there are always solutions that escape the neighborhood of validity of the local normal form analysis. For this reason, the cusp–Hopf bifurcation may be more useful for applications as an organizing center than is the fold–Hopf bifurcation.

1.3. Outline of the paper

The paper is organized as follows. The remainder of Sec. 1 presents the truncated normal form for the cusp–Hopf bifurcation, which has symmetries that facilitate a reduction to a two-dimensional system. Further transformations then simplify the nonlinear coefficients and reduce the number of cases under consideration to just two. The section ends with a discussion of previous and related work.

A detailed analysis of the truncated two-dimensional system is presented in Secs. 2 and 3. In Sec. 2 the invariant sets of the two-dimensional truncated normal form are located, including all equilibrium points and periodic orbits. The main result of Sec. 2 is the determination of three bifurcation varieties in the parameter space, which

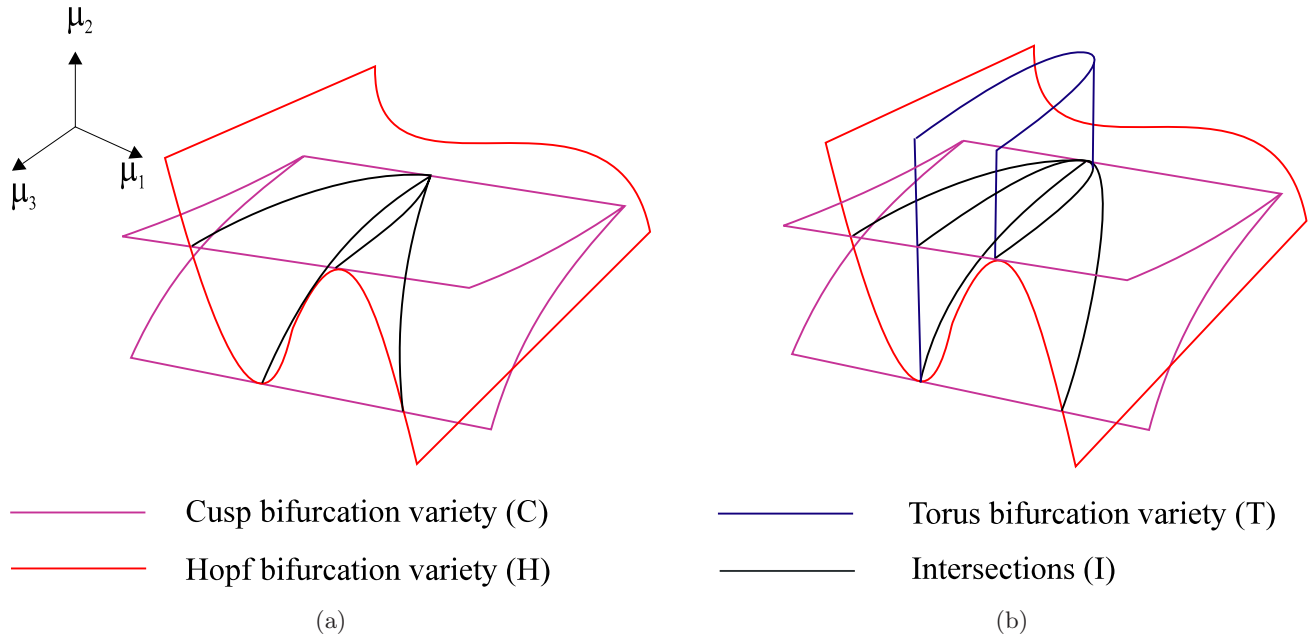


Fig. 3. Bifurcation varieties C , H and T in the parameter space. (a) $k = +1$: periodic solution exists below H . (b) $k = -1$: periodic solution exists above H .

we call Cusp, Hopf and Torus varieties, shown in Fig. 3. This figure is the “organizing center” for the entire paper. In Sec. 3 the study of these bifurcation varieties in the three-dimensional parameter space is reduced to three two-parameter cross-sections, containing codimension-one bifurcation curves and codimension-two bifurcation points. Analysis of neighborhoods of these codimension-two points reveals that all four basic cases of the classical fold–Hopf bifurcation exist in the unfoldings of the cusp–Hopf case. Additional “global” and “trivial” codimension-two bifurcations occur. Phase plane methods are used to obtain the full dynamics of the truncated two-dimensional system, for parameter values near the cusp–Hopf bifurcation point. An interesting *fold-heteroclinic loop* bifurcation in the two-dimensional system leads to a bursting oscillation in the three-dimensional system.

Reconstruction of the dynamics for the three-dimensional vector field, from the results for the two-dimensional (r, z) system, is presented in Sec. 4. Numerical calculations for the three-dimensional system based on the results of Sec. 2 confirm that there is bistability involving an equilibrium point and an invariant torus. On some parameter sets, bursting oscillations can be observed numerically, as predicted by the two-dimensional analysis in Sec. 3. Further aspects of the three-dimensional dynamics as well as suggestions for further work and conclusions are discussed in Sec. 5.

1.4. The normal form

This paper uses the detailed information available for the case of fold–Hopf bifurcation, see [Gavrilov, 1978; Guckenheimer, 1980; Kuznetsov, 2004; Wiggins, 1990], and generalizes it to the cusp–Hopf case. Returning to Eq. (1), henceforth assume that at $\mu = 0$ there exists an equilibrium $x = 0$ satisfying the Hopf eigenvalue condition $\lambda_{1,2} = \pm i\omega$, $\omega > 0$, and the fold condition $\lambda_3 = 0$, where $\lambda_{1,2,3}$ are simple eigenvalues of the linearization $(\partial f / \partial x)(0, 0)$ (Jacobian matrix), and no other eigenvalues have zero real part. If the dimension of the state-space of Eq. (1) is greater than three, then there exists a center manifold of dimension three, corresponding to these three nonhyperbolic eigenvalues. Assuming that a center manifold reduction has been performed, for the rest of this paper we consider system (1) with a three-dimensional state space ($n = 3$) and we write $x = (x_1, x_2, x_3)^T$. The next step is to transform this three-dimensional system to its Poincaré normal form, consisting of the “Poincaré resonant terms”, which lie in a complement of the range of the homological operator of the linearization $(\partial f / \partial x)(0, 0)$ of (1). Since the cusp–Hopf and fold–Hopf bifurcations have the same linearizations, this is just the standard fold–Hopf normal form, given for example in [Chow *et al.*, 1994; Guckenheimer & Holmes, 1986; Iooss & Adelmeyer, 1992; Kuznetsov, 2004; Wiggins, 1990]. The notation of

[Guckenheimer & Holmes, 1986] is followed here,

$$\begin{aligned}\dot{x}_1 &= \gamma x_1 - \omega x_2 + a_1 x_1 x_3 - c_1 x_2 x_3 \\ &\quad + a_2 x_1 (x_1^2 + x_2^2) - c_2 x_2 (x_1^2 + x_2^2) + a_3 x_1 x_3^2 \\ &\quad - c_3 x_2 x_3^2 + O(\|(x_1, x_2, x_3)\|^4) \\ \dot{x}_2 &= \gamma x_2 + \omega x_1 + a_1 x_2 x_3 + c_1 x_1 x_3 \\ &\quad + a_2 x_2 (x_1^2 + x_2^2) + c_2 x_2 (x_1^2 + x_2^2) + a_3 x_2 x_3^2 \\ &\quad + c_3 x_1 x_3^2 + O(\|(x_1, x_2, x_3)\|^4) \\ \dot{x}_3 &= \beta + b_1 (x_1^2 + x_2^2) + b_2 x_3^2 + b_3 x_3^3 \\ &\quad + b_4 (x_1^2 + x_2^2) x_3 + O(\|(x_1, x_2, x_3)\|^4),\end{aligned}\quad (5)$$

where γ, β are the classical fold-Hopf bifurcation (or unfolding) parameters near zero and $a_{1,2,3}, b_{1,2,3,4}, c_{1,2,3}$ are the resonant nonlinear coefficients, depending on μ . It is assumed that the relationship of γ, β to the original parameters μ is such that the Jacobian matrix $\partial(\gamma, \beta)/\partial\mu$ has rank 2. The remainder terms here are all $O(\|(x_1, x_2, x_3)\|^4)$, provided that the vector field $f(x, \mu)$ is C^4 in a neighborhood of $(0, 0)$, by the Taylor remainder theorem. The analysis is simplified by transforming to cylindrical coordinates (r, θ, z) , with $x_1 = r \cos \theta$, $x_2 = r \sin \theta$, $x_3 = z$, and the fold-Hopf normal form becomes

$$\begin{aligned}\dot{r} &= \gamma r + a_1 r z + a_2 r^3 + a_3 r z^2 + O(\|r, z\|^4) \\ \dot{z} &= \beta + b_1 r^2 + b_2 z^2 + b_3 z^3 + b_4 r^2 z + O(\|r, z\|^4) \\ \dot{\theta} &= \omega + c_1 z + c_2 r^2 + c_3 z^2 + O(\|r, z\|^3).\end{aligned}\quad (6)$$

The standard nondegeneracy condition in the analysis of the fold-Hopf normal form is, at $\mu = 0$,

$$a_1 b_1 b_2 \neq 0. \quad (7)$$

In particular, the nondegeneracy of the fold bifurcation corresponds to $b_2 \neq 0$, and then, whenever $\beta b_2 < 0$, there are two equilibrium points of (6) near zero given to leading order by

$$r = 0, \quad z = \pm \sqrt{-\frac{\beta}{b_2} + \dots}. \quad (8)$$

These two equilibria coalesce and vanish as β passes through zero; this is the classical fold (saddlenode) bifurcation.

In this paper it is assumed that the fold bifurcation theorem fails and is replaced by a cusp bifurcation; that is, in (5) and (6) condition (7) is replaced by

$$b_2 = 0, \quad a_1 b_1 b_3 \neq 0. \quad (9)$$

Then the expression (8) for fold equilibrium points is undefined. The singularity is more degenerate

when (9) holds, requiring a minimum of three parameters for its unfolding. Let us formally define the *cusp-Hopf normal form* as

$$\begin{aligned}\dot{r} &= \gamma r + a_1 r z + a_2 r^3 + a_3 r z^2 + O(\|r, z\|^4) \\ \dot{z} &= \beta + \alpha z + b_1 r^2 + b_3 z^3 + b_4 r^2 z + O(\|r, z\|^4) \\ \dot{\theta} &= \omega + c_1 z + c_2 r^2 + c_3 z^2 + O(\|r, z\|^3),\end{aligned}\quad (10)$$

where α, β, γ are unfolding parameters and the Jacobian matrix $\partial(\alpha, \beta, \gamma)/\partial\mu$ is assumed to have rank 3. Justification for this choice is given in the next section. Other choices are possible; for example, [Gavrilov & Roschin, 1983; Gavrilov, 1987] chose a different but equivalent normal form, see Sec. 1.7.

The only θ dependence in Eqs. (10) is in the higher order remainder terms, which are $O(\|r, z\|^k)$ with k as indicated, uniformly in θ for $0 \leq \theta \leq 2\pi$. To begin the analysis, truncate these higher order terms in (10) and observe that the truncated (\dot{r}, \dot{z}) equations are then decoupled from the $\dot{\theta}$ equation in (10). This is due to the S^1 phase-shift symmetry that is a standard consequence of the Hopf bifurcation. Therefore, investigate the following planar truncated system (independent of θ)

$$\begin{aligned}\dot{r} &= r(\gamma + a_1 z + a_2 r^2 + a_3 z^2) \\ \dot{z} &= \beta + \alpha z + b_1 r^2 + b_3 z^3 + b_4 r^2 z.\end{aligned}\quad (11)$$

The planar system (11) inherits a \mathbb{Z}_2 (pitchfork) symmetry from the S^1 phase-shift symmetry; it is invariant under $(r, z) \rightarrow (-r, z)$. Any solution $(r(t), z(t))$ with $r > 0$ of this system may be substituted into the truncated $\dot{\theta}$ equation in (10) and integrated to give

$$\begin{aligned}\theta(t) &= \theta(0) + \omega t + \int_0^t (c_1 z(s) \\ &\quad + c_2 r(s)^2 + c_3 z(s)^2) ds.\end{aligned}\quad (12)$$

Thus, the solutions of the truncation of the three-dimensional normal form (10) are completely determined by the solutions of the planar system (11). The effects of the higher order terms can be understood more easily after the behavior of solutions of (11) is known. It is clear from (11), (12) that, in a neighborhood of $(r, z) = (0, 0)$, $\theta(t)$ is monotone increasing in t (for $\omega > 0$).

1.5. Determinacy and universal unfoldings

Two concepts which play an important role in understanding normal forms are *determinacy* and

versality. In our context, *determinacy* means that the higher order terms truncated in going from Eq. (10) to (11), (12) can be transformed away by an invertible change of variables, in such a way that the dynamics of the solutions of (10) and (11), (12) are qualitatively the same (in the sense of topological equivalence). Nothing essential has been lost in the truncation. Similarly, *versality* means, in our context, that given any three-dimensional parameterized system (1) that has a cusp–Hopf bifurcation at some point of the parameter space, in a neighborhood of that bifurcation point its phase portraits can be mapped onto phase portraits of our parameterized normal form equations, and that map is a homeomorphism in the state variables, preserves the sense of time, and is smooth in the parameters. In other words, *versality* says that the parameterized family of normal form equations captures all of the possible dynamics, sufficiently near the bifurcation point. In this setting, *codimension* may be defined as the minimum number of parameters that gives a versal unfolding, and a *universal unfolding* is a parameterized family that is versal and also has the minimum number of parameters.

Determinacy and versality both were established for a restricted version of the cusp–Hopf bifurcation problem in [Langford, 1984a], see also [Dangelmayr & Armbruster, 1983; Golubitsky & Schaeffer, 1985]. In [Langford, 1984a] the Liapunov–Schmidt method was used to reduce Eq. (1) near a cusp–Hopf bifurcation point to a pair of bifurcation equations of the form

$$\begin{aligned} a(r^2, z, \mu)r &= 0 \\ b(r^2, z, \mu) &= 0. \end{aligned} \quad (13)$$

Solutions (r, z) of this system with $r = 0$ correspond to equilibrium points and solutions with $r > 0$ correspond to periodic orbits of the original system (1). Using equivariant singularity theory, it was shown that if

$$\begin{aligned} b_{zz}(\mathbf{0}) &= 0, & a_z(\mathbf{0}) &\neq 0, \\ b_{r^2}(\mathbf{0}) &\neq 0, & b_{zzz}(\mathbf{0}) &\neq 0, \end{aligned}$$

holds in (13), then at $\mu = 0$ it is \mathbb{Z}_2 -equivalent to the normal form

$$\begin{aligned} zr &= 0 \\ \epsilon_1 r^2 + \epsilon_2 z^3 &= 0, \end{aligned} \quad (14)$$

where $\epsilon_j = \pm 1$ (Proposition 4.2 in [Langford, 1984a]). Furthermore, a universal \mathbb{Z}_2 -unfolding of

(14) is given by

$$\begin{aligned} (\gamma + z)r &= 0 \\ \beta + \alpha z + \epsilon_1 r^2 + \epsilon_2 z^3 &= 0, \end{aligned} \quad (15)$$

where α, β, γ are universal unfolding parameters (Proposition 5.2 in [Langford, 1984a]). Thus, in so far as equilibrium points and periodic orbits are concerned, the determinacy and unfolding problems are solved and the codimension is three. Note that these unfolding parameters are the same as those assumed in (10).

However, determinacy and versality fail in the context of more complex dynamic behavior, such as invariant tori and chaos, which escape the Liapunov–Schmidt analysis. This is because both the existence of the invariant torus and the type of dynamics on the invariant torus are very sensitive to the effects of higher-order terms that have been truncated in going to (11), (12). These higher order terms in general break the S^1 symmetry of (11), (12), which may produce a qualitative change in the dynamics, no matter how small they are quantitatively. These issues are discussed further in Secs. 3 and 4.

The normal form Eqs. (10) may be further simplified. In the planar truncated system (11) there are four cubic terms, of which only the z^3 term remains in the Liapunov–Schmidt normal form (15). In fact, it is possible to eliminate all of the other three cubic terms also in (11) by a near-identity transformation used by Guckenheimer and Gavrilov in the fold–Hopf case, see [Gavrilov, 1987; Gavrilov & Roschin, 1983; Guckenheimer & Holmes, 1986; Kuznetsov, 2004]. Define

$$\begin{aligned} s &= r(1 + gz) \\ w &= z + hr^2 + jz^2 \\ \tau &= \frac{t}{1 + kz}, \end{aligned} \quad (16)$$

where g, h, j, k are coefficients to be determined. Substitution of (16) into (11) leaves the linear and quadratic terms unchanged, and introduces new expressions for the four cubic coefficients in (11), which are linear in g, h, j, k . These expressions have rank three, so values of g, h, j, k can be found to eliminate three, but not all four, of the cubic coefficients. It is possible to eliminate all but the z^3 term and leave the coefficient b_3 of z^3 unchanged. See [Gavrilov & Roschin, 1983; Guckenheimer & Holmes, 1986; Kuznetsov, 2004; Wiggins, 1990] for more details. New higher order terms also appear, which we discard, for consistency

with our earlier truncation. The result is (with a_1, b_1, b_3 unchanged)

$$\begin{aligned}\dot{r} &= (\gamma + a_1 z)r \\ \dot{z} &= \beta + \alpha z + b_1 r^2 + b_3 z^3.\end{aligned}\quad (17)$$

This is consistent with (15). Henceforth assume (11) has been reduced to (17).

A more systematic use of hypernormal forms is given in [Algaba *et al.*, 1998] to simplify additional nonlinear terms in the normal form.

1.6. The normalized 2-D normal form

Equation (17) depends on six parameters: the three unfolding parameters and three parameters that are coefficients of the remaining resonant nonlinear terms. In (17) assume as in (9) that each of resonant terms does not vanish,

$$a_1 b_1 b_3 \neq 0. \quad (18)$$

Now normalize these three coefficients to ± 1 by rescaling the time and state variables by $\bar{t} = \sigma t$, $\bar{r} = \epsilon r$ and $\bar{z} = \delta z$; with $\sigma > 0$, $\epsilon > 0$ and $\delta > 0$ determined by

$$\sigma = \frac{a_1^2}{|b_3|}, \quad \delta = \left| \frac{b_3}{a_1} \right|, \quad \epsilon = \delta \sqrt{\left| \frac{b_1}{a_1} \right|}. \quad (19)$$

Define

$$\begin{aligned}\mu_1 &= \frac{\gamma}{\sigma}, \quad \mu_2 = \frac{\beta\delta}{\sigma}, \quad \mu_3 = \frac{\alpha}{\sigma}, \\ k &= \text{sgn}(b_1) = \pm 1, \\ l &= \text{sgn}(b_3) = \pm 1, \\ m &= \text{sgn}(a_1) = \pm 1.\end{aligned}\quad (20)$$

Substituting and dropping the overbars, we have replaced (17) by

$$\begin{aligned}\dot{r} &= r(\mu_1 + mz) \\ \dot{z} &= \mu_2 + \mu_3 z + kr^2 + lz^3.\end{aligned}\quad (21)$$

The system (21) represents eight cases, depending on the signs of $k = \pm 1$, $l = \pm 1$, $m = \pm 1$. However, system (21) is unchanged by the transformation

$$\{z, t, \mu_1, \mu_3, l\} \rightarrow \{-z, -t, -\mu_1, -\mu_3, -l\}. \quad (22)$$

Thus any case with $l = +1$ may be transformed to one with $l = -1$, under the reflection (22). The most significant effect of (22) is to reverse stabilities (i.e. $t \rightarrow -t$). The phase portrait for any case

with $l = +1$ may be obtained from the corresponding one under (22) by reflecting z and reversing the direction of time t . In the case $l = -1$ the equilibria on the cusp manifold have stabilities as indicated in Fig. 1, ignoring the Hopf bifurcation. This is the case that is most relevant for physical applications. Therefore in this paper, only the cases with $l = -1$ are investigated, without loss of generality.

Similarly, one need only consider $m = +1$ in (21), since (21) is also invariant under the reflection

$$\{z, \mu_2, k, m\} \rightarrow \{-z, -\mu_2, -k, -m\}. \quad (23)$$

If $m = -1$ then one can apply (23) and obtain $m = +1$. Combining these transformations reduces eight cases to two. Therefore, assume without loss of generality

$$k = \pm 1, \quad l = -1, \quad m = +1, \quad (24)$$

and write the planar truncated normal form (21) as

$$\begin{aligned}\dot{r} &= r(\mu_1 + z) \\ \dot{z} &= \mu_2 + \mu_3 z + kr^2 - z^3, \quad k = \pm 1.\end{aligned}\quad (25)$$

For explicit solutions in all eight cases without exploiting these reflectional symmetries, see [Harlim, 2001]. Equation (25) is the focus of the analysis in Sec. 2.

1.7. Relationship to previous work

This paper is a contribution to the growing literature on codimension-three bifurcations of vector fields. In four dimensions, resonant Hopf bifurcations have been studied by Vanderbauwhede [1986]; van Gils *et al.* [1990]; LeBlanc and Langford [1996]; Govaerts *et al.* [1997]; Langford and Zhan [1999]. In three dimensions in addition to the zero-Hopf case of this paper, bifurcation at a triple zero eigenvalue has been studied widely, for example in [Freire *et al.*, 2002; Sieber & Krauskopf, 2004]. In two dimensions, the various cases of codimension-three Hopf bifurcations were analyzed in [Golubitsky & Langford, 1981] and degenerate Bogdanov–Takens bifurcations have been explored by many authors, see [Kuznetsov, 2005] and further references therein.

Previous work on the cusp–Hopf bifurcation includes proofs by methods of equivariant singularity theory of determinacy and versality for the two-dimensional normal form (21) as described in Sec. 1.5; see [Dangelmayr & Armbruster, 1983; Golubitsky & Schaeffer, 1985; Langford, 1984a]. Complementary numerical studies in [Langford,

1983, 1984b] of the three-dimensional system have revealed more complex behavior that is beyond the range of singularity theory methods, such as invariant tori, phase locking, period doubling, bursting oscillations, strange attractors and transient chaos.

Independently, Gavrilov and Roschin [1983]; Gavrilov [1987] performed a normal form analysis of the cusp–Hopf bifurcation. The physically interesting stable case corresponding to $b_2 = 0$, $b_3 < 0$, $a_1 b_1 < 0$ was identified in the context of a more general stability analysis in [Gavrilov & Roschin, 1983]. Gavrilov [1987] used a choice of unfolding parameters and a normal form that is equivalent to

$$\begin{aligned}\dot{r} &= rz \\ \dot{\theta} &= \omega + c_1 z + c_2 r^2 + c_3 z^2 + O(\|r, z\|^3) \\ \dot{z} &= \delta + \epsilon z + \mu z^2 + b_1 r^2 + b_3 z^3 + b_4 r^2 z \\ &\quad + O(\|r, z\|^4).\end{aligned}\quad (26)$$

This choice gives a simpler \dot{r} equation than (17), and places all three unfolding parameters in the \dot{z} equation. With Gavrilov’s unfolding parameters δ , ϵ , μ , the equation of the cusp variety (4) takes the form

$$\left(\frac{\delta + \frac{\epsilon\mu}{3} + \frac{2\mu^3}{27}}{2} \right)^2 = \left(\frac{\epsilon + \frac{\mu^2}{3}}{3} \right)^3, \quad (27)$$

which reduces to (4) when $\mu = 0$. However, the unfolding parameters used in the present paper preserve the form of the cusp in Eqs. (3) and (4), and Fig. 1, even with the inclusion of the Hopf bifurcation. The two-dimensional phase portraits presented here in Fig. 10 for the case $k = -1$ are not equivalent to those in [Gavrilov, 1987], as a consequence of Proposition 2.1. The phase portraits for $k = +1$ presented in Fig. 9 have not been published previously. The singular phase portraits for $k = \pm 1$ in Fig. 2 were sketched in [Gavrilov & Roschin, 1983].

Krauskopf and Rousseau [1997] considered a two-dimensional, codimension-three normal form very similar to (11). Their case, like ours, may be obtained from the fold–Hopf normal form (6) but with a different degeneracy in (6)

$$b_1 = 0, \quad a_1 b_2 b_3 \neq 0, \quad (28)$$

that is, the r^2 term is missing instead of the z^2 term in the \dot{z} equation. After some simplifying transformations preserving the \mathbb{Z}_2 symmetry, they show that this singularity is determined (for most a, b) by

its four-jet

$$\begin{aligned}\dot{r} &= -ar z - r^3 \\ \dot{z} &= -z^2 + br^4\end{aligned}\quad (29)$$

and they analyze its natural unfolding (analogous to (21))

$$\begin{aligned}\dot{r} &= \mu_1 r - ar z - r^3 \\ \dot{z} &= \mu_2 + \mu_3 r^2 - z^2 + br^4.\end{aligned}\quad (30)$$

Algaba *et al.* [1998] presented a detailed analysis of the fold–Hopf normal form, using C^∞ -equivalence to obtain a hypernormal form. They provided recursive algorithms for efficient computation of the coefficients. This work will facilitate the study of degenerate fold–Hopf bifurcations in applications.

2. Equilibria and Periodic Orbits in \mathbb{R}^2

This section presents the study of equilibrium points and periodic orbits and their bifurcations for the two-dimensional truncated normal form (25). In Sec. 2.1 we determine the equilibria and their bifurcation varieties. Hopf bifurcation analysis in Sec. 2.2 determines the periodic cycles of (25) and their stability properties.

The analysis begins with the codimension-three singularity (organizing center) $\mu_1 = \mu_2 = \mu_3 = 0$, where the 2D normal form (25) is

$$\begin{aligned}r' &= rz \\ z' &= kr^2 - z^3.\end{aligned}\quad (31)$$

The singular phase portraits for $k = \pm 1$ are in Fig. 2. The remaining six of the eight phase portraits for $k = \pm 1$, $l = \pm 1$, $m = \pm 1$, are easily obtained from these two using the symmetries (22) and (23); that is, by reversing $t \rightarrow -t$ or $z \rightarrow -z$, or both. The origin is asymptotically stable only for $(k, l, m) = (-1, -1, 1)$ [as in Fig. 2(b)] and $(1, -1, -1)$ [obtained from $z \rightarrow -z$ in Fig. 2(b)].

In both phase portraits of Fig. 2 there exists a separatrix orbit with the property that as $t \rightarrow -\infty$, all orbits above (below) the separatrix satisfy $z \rightarrow +\infty$ ($-\infty$). The nullclines $z' = 0$ are given by the two curves $z = kr^{\frac{2}{3}}$, $k = \pm 1$. Define region R by

$$R = \left\{ (r, z) \mid -r^{\frac{2}{3}} - \frac{2}{9} < z < -r^{\frac{2}{3}} \right\}. \quad (32)$$

Proposition 2.1. *In the case $k = -1$, there exists a unique separatrix orbit S in R , for which any solution orbit of (31) with initial point above (below) S stays above (below) S for all t and as $t \rightarrow \infty$ approaches $(0, 0)$ tangent to S .*

Proof. Define $V(r, z) = r^2 + z^3$. Then $\dot{V}(r, z) \equiv V_r \cdot r' + V_z \cdot z'$ satisfies $\dot{V} < 0$ ($\dot{V} > 0$) at every point on the upper (lower) boundary of R . Thus R is positively invariant. No solution orbit can cross through R and every orbit with $r > 0$ eventually enters R . To show there is a unique orbit that remains in R for all $t \in \mathbb{R}$, suppose there exist two such orbits, $S_1 \neq S_2$. Then a vertical line L with fixed $r > 0$ intersects orbits S_1, S_2 at two points with $z_1 \neq z_2$ in R . But a calculation shows that the slope dz/dr is strictly decreasing with z on L . Therefore, the orbits S_1, S_2 strictly diverge with increasing r at each such L . Since L in R has finite length $\frac{2}{9}$, one of S_1, S_2 must leave R as $t \rightarrow -\infty$. By contradiction, $S_1 = S_2$ and there exists a unique separatrix orbit S in R . ■

The proof for the case $k = +1$ is similar except the nullcline is $z = +r^{\frac{2}{3}}$ and the separatrix approaches $(0, 0)$ as $t \rightarrow -\infty$. Region R in (32) is due to A. Willms [private communication]. The phase portraits of Figs. 2(a) and 2(b) are sketched in [Gavrilov & Roschin, 1983] but for the case $k = -1$ the separatrix S and the infinite family of orbits coming from $z = -\infty$ are missing.

2.1. Equilibria in \mathbb{R}^2

Equilibrium points of (25) on the z -axis ($r = 0$) are independent of $k = \pm 1$, and given by

$$\begin{aligned} r &= 0 \\ \mu_2 + \mu_3 z - z^3 &= 0. \end{aligned} \quad (33)$$

The second equation of (33) recovers exactly the *cusp manifold* M of Eq. (3) and Fig. 1. For (μ_2, μ_3) inside the cusp, denote the three equilibria by $E_1 = (0, z_1)$, $E_2 = (0, z_2)$, $E_3 = (0, z_3)$; outside the cusp there is exactly one equilibrium $E_1 = (0, z_1)$. The coordinates of these equilibria are given explicitly by the following expressions when they are real. Define S^+ and S^- by

$$S^\pm = \left[\frac{\mu_2}{2} \pm \sqrt{\left(\frac{\mu_2}{2}\right)^2 - \left(\frac{\mu_3}{3}\right)^3} \right]^{1/3}, \quad (34)$$

then E_1, E_2, E_3 are given by

$$\begin{aligned} z_1 &= S^+ + S^- \\ z_2 &= -\frac{1}{2}(S^+ + S^-) + i\frac{\sqrt{3}}{2}(S^+ - S^-) \\ z_3 &= -\frac{1}{2}(S^+ + S^-) - i\frac{\sqrt{3}}{2}(S^+ - S^-). \end{aligned} \quad (35)$$

Note that z_1 is real for *all* values of μ_2, μ_3 .

Besides these equilibria with $r = 0$ there is a nontrivial equilibrium of (25) with $r \neq 0$, which we denote $E_4 = (r_4, z_4)$, where

$$z_4 = -\mu_1, \quad r_4^2 = k[-\mu_2 + \mu_3\mu_1 - \mu_1^3], \quad (36)$$

whenever the expression on the right is positive. Restoring θ , Eq. (12) yields a periodic orbit in the three-dimensional space with amplitude $r > 0$, corresponding to the original primary Hopf bifurcation. Since the normal form is symmetric under $r \rightarrow -r$, this is a pitchfork bifurcation in (25), but because r is a polar coordinate the solution with $r < 0$ is discarded. With μ_2 as bifurcation parameter, this bifurcation is supercritical (subcritical) for $k = -1$ ($k = +1$).

Thus there are up to four equilibrium points of (25). The above expressions (34)–(36) determine bifurcation varieties, where the expressions for equilibria change from real to complex. They are

$$C = \left\{ (\mu_1, \mu_2, \mu_3) \mid \left(\frac{\mu_2}{2}\right)^2 - \left(\frac{\mu_3}{3}\right)^3 = 0 \right\}, \quad (37)$$

$$H = \{(\mu_1, \mu_2, \mu_3) \mid \mu_2 - \mu_3\mu_1 + \mu_1^3 = 0\}. \quad (38)$$

Note that the algebraic variety C is a trivial extension to three parameters of the *cusp bifurcation variety* in the two-parameter plane given earlier in (4). We call H the *Hopf bifurcation variety* because it corresponds to primary Hopf bifurcation points for the three-dimensional dynamics. Both C and H are shown in Fig. 3.

2.2. Secondary Hopf bifurcation in \mathbb{R}^2

The nontrivial equilibrium $E_4 = (r_4, z_4)$ in (36) may undergo a *secondary Hopf bifurcation*. This section gives a proof of the existence of a secondary Hopf bifurcation for Eq. (25), verifies the crossing condition and determines the Liapunov number. Numerical verification that this secondary bifurcation corresponds to a torus (Neimark–Sacker) bifurcation in the three-dimensional system is presented in Sec. 4.

Linearization of (25) at E_4 gives the Jacobian

$$A = \begin{pmatrix} 0 & r_4 \\ 2kr_4 & \mu_3 - 3\mu_1^2 \end{pmatrix}, \quad (39)$$

which has eigenvalues $\lambda(\mu) = \alpha(\mu) \pm i\beta(\mu)$ given by

$$\alpha(\mu) = \frac{1}{2}(\mu_3 - 3\mu_1^2) \quad (40)$$

$$\beta(\mu) = \frac{1}{2}\sqrt{-\mu_3^2 + 6\mu_3\mu_1^2 - 9\mu_1^4 - 8[-\mu_2 + \mu_3\mu_1 - \mu_1^3]}.$$

The Hopf existence theorem requires $\alpha = 0$ and $\beta \neq 0$ or equivalently

$$\operatorname{tr}(A) = \mu_3 - 3\mu_1^2 = 0 \quad \text{and} \quad \det A = -2kr_4^2 > 0. \quad (41)$$

Thus, a necessary condition for secondary Hopf bifurcation is

$$\mu_3 = 3\mu_1^2 \quad \text{and} \quad k = -1. \quad (42)$$

When (41) and (42) hold, A has imaginary eigenvalues $\pm i\beta(\mu_0)$ given by

$$\beta(\mu_0) = \sqrt{2r_4^2} = \sqrt{2\mu_2 - 4\mu_1^3}, \quad (43)$$

and for this to be real, $\mu_2 > 2\mu_1^3$, which leads to the following proposition.

Proposition 2.2. *Consider system (25) with $k = \pm 1$, $l = -1$, $m = +1$, and with a nontrivial equilibrium point E_4 . Then a classical Hopf bifurcation occurs generically at the equilibrium E_4 , iff $k = -1$. This Hopf bifurcation occurs on crossing the bifurcation variety*

$$T = \{(\mu_1, \mu_2, \mu_3) | \mu_3 = 3\mu_1^2, \mu_2 > 2\mu_1^3\}, \quad (44)$$

see Fig. 3. If μ_3 is chosen as the bifurcation parameter, then the Hopf bifurcation is supercritical; that is, a stable periodic orbit appears on crossing toward the inside of the parabolic semi-cylinder defined by (44).

(The set (44) is denoted T , as it represents a *Torus bifurcation* in 3D.)

Proof. It was shown above that E_4 is real and has purely imaginary eigenvalues, if and only if $k = -1$ and (44) holds. Let μ_3 be the bifurcation parameter on crossing T . Hopf's crossing condition from (40) is

$$\frac{\partial \alpha(\mu)}{\partial \mu_3} = \frac{1}{2} > 0, \quad (45)$$

so the crossing condition is always satisfied with μ_3 as parameter.

To complete the proof of Hopf bifurcation, it is necessary to verify that the Liapunov number $L_1(0)$ (the cubic coefficient in the normal form for Hopf bifurcation) is nonzero. $L_1(0)$ may be computed from the following formula given in [Guckenheimer & Holmes, 1986]

$$\begin{aligned} L_1(0) = & \frac{1}{16} [f_{xxx} + f_{xyy} + g_{xxy} + g_{yyy}] \\ & + \frac{1}{16\omega} [f_{xy}(f_{xx} + f_{yy}) - g_{xy}(g_{xx} + g_{yy}) \\ & - f_{xx}g_{xx} + f_{yy}g_{yy}]. \end{aligned} \quad (46)$$

Here f and g are from the Hopf normal form ($\mu = 0$) in Cartesian coordinates

$$\begin{aligned} \dot{x} &= -\beta(0)y + f(x, y, 0) \\ \dot{y} &= \beta(0)x + g(x, y, 0). \end{aligned} \quad (47)$$

The calculation of $L_1(0)$ may be found in [Harlim, 2001], where it is shown that

$$L_1 = \frac{3}{8}l, \quad (48)$$

which is negative when $l = -1$ as assumed here. This with (45) implies that the Hopf bifurcation is *supercritical* in μ_3 , that is to the *inside* of T in (44). ■

One may instead choose μ_1 as bifurcation parameter, with crossing condition

$$\frac{\partial \alpha(\mu)}{\partial \mu_1} = -3\mu_1 \neq 0, \quad (49)$$

or simply $\mu_1 \neq 0$. This derivative obviously changes sign with μ_1 , which again implies that the direction of bifurcation is to the inside of the parabolic semi-cylinder (44). The Hopf bifurcation with parameter μ_1 , at $\mu_1 = 0$ in the plane $\mu_3 = 0$, is a type of *degenerate Hopf bifurcation* that was analyzed in [Golubitsky & Langford, 1981]. The results of [Golubitsky & Langford, 1981] are applied in a neighborhood of $\mu_1 = 0$ in Sec. 3.2. Parameter μ_2 is never a good choice of Hopf bifurcation parameter.

Note that the closures of C , H and T meet in the curves I shown in Fig. 3, and I contains the zero-Hopf bifurcation curve defined by

$$ZH = \{(\mu_1, \mu_2, \mu_3) | \mu_3 = 3\mu_1^2, \mu_2 = 2\mu_1^3\}. \quad (50)$$

In Sec. 3.3 the interesting behavior in a neighborhood of ZH is explored.

3. Codimension-Two Bifurcations in \mathbb{R}^2

This section presents a more detailed study of the codimension-two bifurcations that exist locally in Fig. 3, where C , H and T meet. The generic properties of local codimension-one and two bifurcations can be found in standard texts, such as [Guckenheimer & Holmes, 1986; Kuznetsov, 2004; Wiggins, 1990].

In all cases, the bifurcation varieties C , H and T of Fig. 3 intersect transversely any plane $\mu_3 = \text{constant} \neq 0$. Furthermore, the curves of intersection in this plane remain topologically equivalent as $\mu_3 \neq 0$ varies continuously. Thus, it is sufficient as well as convenient to study the behavior in Fig. 3

by taking three two-dimensional slices, corresponding to $\mu_3 = -\epsilon$, $\mu_3 = 0$ and $\mu_3 = +\epsilon$, respectively, for small $\epsilon > 0$. The following Secs. 3.1–3.3 explore each of these three cases, assuming $k = \pm 1$, $l = -1$, $m = +1$.

3.1. Negative μ_3

For fixed $\mu_3 < 0$, Eq. (25) has a unique equilibrium on the z -axis, $E_1 = (0, z_1)$ as in (35), and possibly an equilibrium with $r > 0$, $E_4 = (r_4, z_4)$, see (36). The Jacobian matrix of (25) at general (r, z) is

$$J = \begin{pmatrix} \mu_1 + z & r \\ 2kr & \mu_3 - 3z^2 \end{pmatrix}, \quad (51)$$

which becomes at E_1 and E_4 respectively

$$\begin{aligned} J_1 &= \begin{pmatrix} \mu_1 + z_1 & 0 \\ 0 & \mu_3 - 3z_1^2 \end{pmatrix}, \\ J_4 &= \begin{pmatrix} 0 & r_4 \\ 2kr_4 & \mu_3 - 3\mu_1^2 \end{pmatrix}. \end{aligned} \quad (52)$$

When $\mu_3 < 0$, the determinant of J_1 or of J_4 can be zero if and only if

$$\mu_2 - \mu_1\mu_3 + \mu_1^3 = 0, \quad (53)$$

which is the Hopf bifurcation variety H in (38). Elementary calculations show that the 2D phase portraits on each side of H , including the equilibria and their stabilities, are as shown in Fig. 4.

3.2. Zero μ_3

The bifurcations and phase portraits for the case $\mu_3 = 0$ are similar to those shown in Fig. 4, except

that H is now tangent to the μ_1 axis at $(0, 0)$ and there is an additional bifurcation variety in the case $k = -1$, given by the semi-axis $\{\mu_2 > 0, \mu_1 = 0, \mu_3 = 0\}$, which is tangent to T and on which there is a degenerate Hopf bifurcation (the Hopf crossing condition is violated).

In Fig. 3(b), consider the intersection of any horizontal plane, defined by a constant $\mu_2 > 0$, with a spherical neighborhood of a point on the μ_2 -axis. This yields a small disk that intersects the torus bifurcation variety T of Fig. 3(b) in a U-shaped curve. (Because the disk should not intersect the cusp bifurcation variety C , the disk must shrink to zero as $\mu_2 \rightarrow 0$; see Fig. 3(b).) Now in this disk consider a line $\mu_3 = \text{constant}$ with μ_1 varying as bifurcation parameter. This line intersects T in two points if $\mu_3 > 0$, one point if $\mu_3 = 0$ and no point if $\mu_3 < 0$. This type of degenerate Hopf bifurcation has been studied in [Golubitsky & Langford, 1981], see also [Golubitsky & Schaeffer, 1985].

Proposition 3.1. *Consider a line with fixed μ_2, μ_3 , both positive, and with μ_1 varying. Then, for each sufficiently small (μ_2, μ_3) , there exist two Hopf bifurcation points, one at each intersection of this line with the U-shaped curve defined by T . The directions of both bifurcating branches are to the interior of the region bounded by T and the periodic orbits are stable limit cycles. Moreover, these two branches are in fact one and the same continuous branch of periodic solutions joining the two Hopf bifurcations on T , and these periodic solutions are unique. As $\mu_3 \rightarrow 0^+$, this branch of periodic*

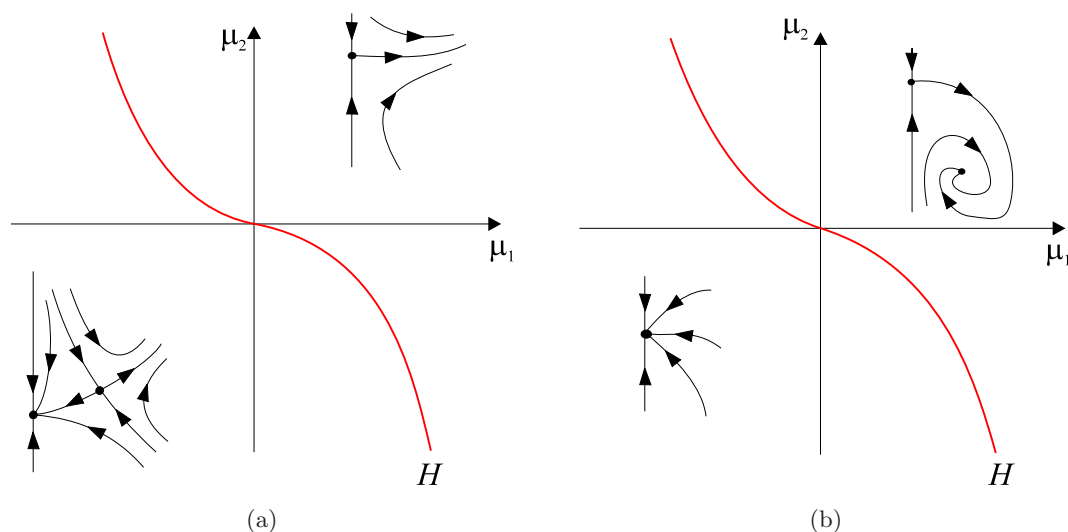


Fig. 4. Bifurcation variety H and phase portraits for $\mu_3 < 0$. (a) $k = +1$: E_4 exists below H as a saddle. (b) $k = -1$: E_4 exists above H as a sink.

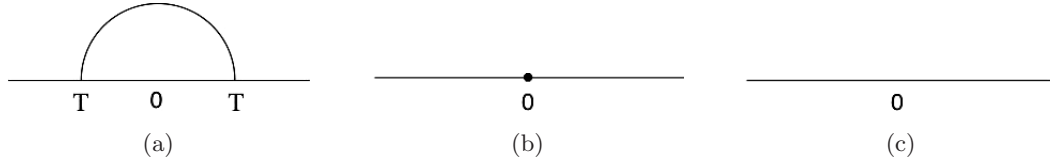


Fig. 5. Degenerate Hopf bifurcation for $k = -1$ and fixed small $\mu_2 > 0$. (a) A unique branch of periodic orbits for $\mu_3 > 0$, parameterized by μ_1 , begins and ends in a classical Hopf bifurcation at T . (b) The branch shrinks to a point for $\mu_3 = 0$. (c) The branch does not exist for $\mu_3 < 0$.

solutions shrinks to a point on the positive μ_1 -axis, and then disappears for $\mu_3 < 0$; see Fig. 5.

Proof. The first two statements of this Proposition follow directly from Proposition 2.2. The last two statements follow from the case of normal form (4.2) in [Golubitsky & Langford, 1981], based on the calculations (49) and (48) and above. ■

This uniqueness result, obtained by application of the theory in [Golubitsky & Langford, 1981] and [Golubitsky & Schaeffer, 1985], yields new information for sufficiently small $\{|\mu_1|, \mu_2 > 0, \mu_3 > 0\}$. Until now, the uniqueness of periodic orbits in this region has been an open question. For example, Gavrilov [1987] assumed uniqueness as an additional hypothesis in order to complete his classification of two-dimensional phase portraits.

3.3. Positive μ_3

In the case $\mu_3 > 0$, much richer dynamics is possible for Eq. (25), due to the existence of the bifurcation varieties C and T in addition to H . These are two-dimensional surfaces in the parameter space that intersect along the curves I in Fig. 3. It is clear that I intersects transversely any plane with fixed

small $\mu_3 > 0$. Denote these points of intersection by ZH (zero-Hopf), HC (Hopf-cusp) and TC (torus-cusp), see Fig. 6(a). The next goal is to understand the dynamics near these codimension-two points, given in parametric form by

$$ZH_1 = \left\{ (\mu_1, \mu_2) \mid \mu_1 = -\sqrt{\frac{\mu_3}{3}}, \mu_2 = -2 \left(\frac{\mu_3}{3} \right)^{3/2} \right\} \quad (54)$$

$$ZH_2 = \left\{ (\mu_1, \mu_2) \mid \mu_1 = +\sqrt{\frac{\mu_3}{3}}, \mu_2 = +2 \left(\frac{\mu_3}{3} \right)^{3/2} \right\} \quad (55)$$

$$HC_1 = \left\{ (\mu_1, \mu_2) \mid \mu_1 = -2\sqrt{\frac{\mu_3}{3}}, \mu_2 = +2 \left(\frac{\mu_3}{3} \right)^{3/2} \right\} \quad (56)$$

$$HC_2 = \left\{ (\mu_1, \mu_2) \mid \mu_1 = +2\sqrt{\frac{\mu_3}{3}}, \mu_2 = -2 \left(\frac{\mu_3}{3} \right)^{3/2} \right\} \quad (57)$$

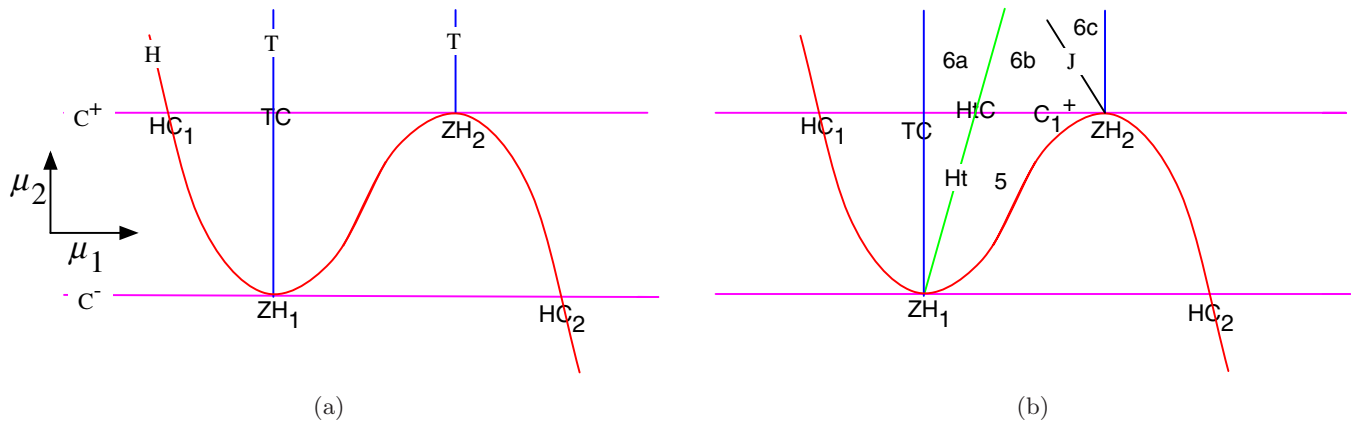


Fig. 6. (a) Codimension-two intersections of the bifurcation varieties C , H , T , in the (μ_1, μ_2) plane for fixed $\mu_3 > 0$, $k = -1$. (b) Same figure with the varieties Ht and J inherited from the fold-Hopf bifurcation theory of [Guckenheimer & Holmes, 1986].

$$TC = \left\{ (\mu_1, \mu_2) \mid \mu_1 = -\sqrt{\frac{\mu_3}{3}}, \right. \\ \left. \mu_2 = +2 \left(\frac{\mu_3}{3} \right)^{3/2} \right\}. \quad (58)$$

3.3.1. Neighborhoods of ZH_1 and ZH_2

We begin by analyzing the neighborhoods of the zero-Hopf points ZH_1 and ZH_2 , which are the most interesting cases. They appear to be highly degenerate in Fig. 6(a). The varieties C and H meet tangentially rather than transversely at ZH_1 and ZH_2 , and furthermore, in the case $k = -1$, the variety T terminates at the same points. These degeneracies are characteristic of the codimension-two fold–Hopf bifurcation, see [Guckenheimer & Holmes, 1986; Wiggins, 1990; Kuznetsov, 2004]. Indeed, we will show that a generic fold–Hopf bifurcation occurs at each of ZH_1 and ZH_2 .

First, translate both the coordinates and the parameters in the cusp–Hopf normal form (25), to bring ZH_1 (or ZH_2) to the origin in parameter space and bring the corresponding fold equilibrium point to the origin in state space. Then determine the Poincaré normal form in these new coordinates and show that it is in fact a nondegenerate fold–Hopf normal form, for fixed $\mu_3 > 0$. Then the classical results of Gavrilov [1978]; Guckenheimer [1980] for this case can be invoked to describe the behavior of system (25), near ZH_1 and ZH_2 .

The parameters at the bifurcation points ZH_1 and ZH_2 are given by (54), (55), and the coordinates of the corresponding equilibria in state space are

$$\begin{aligned} ZH_1 : \quad r &= 0, \quad z_1 = -2\sqrt{\frac{\mu_3}{3}}, \\ z_2 &= z_3 = z_4 = \sqrt{\frac{\mu_3}{3}}, \\ ZH_2 : \quad r &= 0, \quad z_1 = 2\sqrt{\frac{\mu_3}{3}}, \\ z_2 &= z_3 = z_4 = -\sqrt{\frac{\mu_3}{3}}. \end{aligned} \quad (59)$$

In each case, we have a multiple equilibrium point with $r = 0$, $z_2 = z_3 = z_4$, which is a classical codimension-two fold–Hopf bifurcation point. The other equilibrium point $(0, z_1)$ is outside the local neighborhood of the fold–Hopf bifurcation, and thus does not enter into the present analysis. We deal with the two cases (59) simultaneously, by defining

$\sigma = \pm 1$, with $\sigma = +1$ for the case ZH_1 and $\sigma = -1$ for the case ZH_2 . Now translate the multiple equilibrium point to the origin in each case, by letting $\hat{z} = z - \sigma\sqrt{\mu_3/3}$ and substituting into (25), to obtain

$$\begin{aligned} \dot{r} &= \phi_1 r + r \hat{z} \\ \dot{\hat{z}} &= \phi_2 - \sigma\sqrt{3\mu_3} \hat{z}^2 + k r^2 - \hat{z}^3, \end{aligned} \quad (60)$$

where $\phi_1 = \mu_1 + \sigma\sqrt{\mu_3/3}$ and $\phi_2 = \mu_2 + (2\sigma/3)\sqrt{\mu_3/3}$. Simplify these equations by rescaling $\zeta = \sqrt{3\mu_3}\hat{z}$ and $\rho = \sqrt[4]{3\mu_3}r$. Then (60) becomes

$$\begin{aligned} \dot{\rho} &= \lambda_1 \rho + a \rho \zeta \\ \dot{\zeta} &= \sigma \lambda_2 - \zeta^2 + b \rho^2 - f \zeta^3, \end{aligned} \quad (61)$$

where $\lambda_1 = \phi_1$, $\lambda_2 = \phi_2\sqrt{3\mu_3}$, $a = \sigma/\sqrt{3\mu_3}$, $b = \sigma k = \pm 1$ and $f = 1/3\mu_3 > 0$. Equation (61) is the normal form of the fold–Hopf bifurcation, in the version given by Guckenheimer and Holmes [1986]. (An equivalent normal form for the fold–Hopf bifurcation has been studied by Gavrilov [1978] and Kuznetsov [2004]. They retain a different choice of cubic term in their analysis, which is less convenient for the purposes of this paper.)

The local bifurcation diagrams in neighborhoods of ZH_1 and ZH_2 may now be obtained from the fold–Hopf results of Guckenheimer and Holmes [1986]. There are four main cases in [Guckenheimer & Holmes, 1986], depending on the signs of $a = \sigma/\sqrt{3\mu_3}$ and $b = \sigma k$ in (61), and there is a one-to-one correspondence between those four cases and the four choices of signs here of $\sigma = \pm 1$ and $k = \pm 1$; see Table 1. (Since μ_3 is small, we may assume $|a| > 1$ so that in cases II and IV of [Guckenheimer & Holmes, 1986] we fall in subcases IIB and IVb, respectively.) It is remarkable that each of the four basic cases of the fold–Hopf bifurcation in [Guckenheimer & Holmes, 1986] (see also [Kuznetsov, 2004; Langford, 1979; Wiggins, 1990]) occurs *exactly once* among the points ZH_1 and ZH_2 for the two cases $k = \pm 1$ in the cusp–Hopf bifurcation as shown in Table 1.

Figure 6(b) presents the additional information inherited from the fold–Hopf bifurcation, in the neighborhoods of bifurcation points ZH_1 and ZH_2 , for the more interesting case of $k = -1$. In this case, neighborhoods of ZH_1 and ZH_2 include not only the torus bifurcation variety T , but also the possibility of varieties Ht and J , as we now describe. The nontrivial equilibrium $E_4 = (r_4, z_4)$ exists at all points above the variety H in Fig. 6(b), and E_4 undergoes secondary Hopf bifurcation on T . It is

Table 1. Correspondence between the four basic cases of fold–Hopf bifurcation in [Guckenheimer & Holmes, 1986] and the bifurcations at ZH_1 and ZH_2 in the cusp–Hopf case.

Case in GH [1986]	GH Conditions	Signs of σ and k	Cusp–Hopf Case
I	$b = +1, a > 0$	$\sigma = +1, k = +1$	Case: ZH_1, T absent
II	$b = +1, a < 0$	$\sigma = -1, k = -1$	Case: ZH_2, T exists
III	$b = -1, a > 0$	$\sigma = +1, k = -1$	Case: ZH_1, T exists
IV	$b = -1, a < 0$	$\sigma = -1, k = +1$	Case: ZH_2, T absent

known that the Hopf bifurcation on T in the fold–Hopf normal form truncated to quadratic order is degenerate; that is, the equilibrium corresponding to $E_4 = (r_4, z_4)$ is a nonlinear center in this case. The cubic term ζ^3 in (61) removes this degeneracy. According to delicate analysis involving Abelian integrals by several authors, see [Chow *et al.*, 1994; van Gils, 1985; Guckenheimer & Holmes, 1986; Zoladek, 1987], in a neighborhood of ZH_1 (case III, Fig. 7.4.5 in [Guckenheimer & Holmes, 1986]) there is a unique branch of hyperbolic periodic solutions of (61) growing monotonically in amplitude to the right of T and terminating in a *heteroclinic loop bifurcation variety* along Ht in Fig. 6(b), tangent at ZH_1 to the line (with $\mu_3 = \text{constant}$) given by

$$Ht : \mu_2 + 2 \left(\frac{\mu_3}{3} \right)^{3/2} = 4\mu_3 \left[\mu_1 + \left(\frac{\mu_3}{3} \right)^{1/2} \right]. \quad (62)$$

If the coefficient of the cubic term ζ^3 in (61) is negative, as is true with $l = -1$, then the fold–Hopf analysis implies that these periodic orbits are asymptotically stable limit cycles existing uniquely to the right of T , in a wedge between T and Ht , see Fig. 6(b). These conclusions remain valid in a neighborhood of ZH_1 when higher order terms are restored for the cusp–Hopf system. Thus in Fig. 6(b), it remains to determine how far the bifurcation variety Ht persists away from ZH_1 , and if there exists a point of intersection of Ht and C , as indicated by HtC in Fig. 6(b). These issues are addressed in Sec. 3.3.3.

The situation at ZH_2 with $k = -1$ is similar. This corresponds to Case II, Fig. 7.4.4 in [Guckenheimer & Holmes, 1986], with the parameter μ_2 flipped in sign. The bifurcation varieties C and H are locally in agreement with those of the fold–Hopf case. In the quadratic truncation of the fold–Hopf case in (61), T corresponds to a degenerate Hopf bifurcation and there is a nonlinear center with periodic orbits of arbitrarily large amplitude. The cubic term ζ^3 in (61) again removes this degeneracy. In the case $l = -1$ for the fold–Hopf case, a unique branch of stable limit cycles grows

monotonically from E_4 and “blows up”, in the following sense. As the parameters (μ_1, μ_2) move away from T (to the left in Fig. 6(b)) while remaining in a neighborhood of ZH_2 , the limit cycle escapes any small neighborhood of the equilibrium E_4 . There is no heteroclinic loop bounding these limit cycles. (This does not mean that the limit cycle for the original system grows to infinite amplitude, since these results are valid only locally.) The line J in Fig. 6(b) represents this boundary on which the limit cycle “locally blows up” in the fold–Hopf analysis; see Sec. 3.3.3.

The case $k = +1$ in the cusp–Hopf normal form is much simpler than the case $k = -1$ that is shown in Fig. 6(b). For $k = +1$, none of T , Ht and J exist. The bifurcation varieties C and H remain the same as shown in Fig. 6. The nontrivial equilibrium E_4 exists, everywhere *below* H in these figures, and is a saddle point (thus there can be no secondary Hopf bifurcation from E_4). As in Table 1, there is a neighborhood of ZH_1 agreeing with Case I, Fig. 7.4.3 in [Guckenheimer & Holmes, 1986], and a neighborhood of ZH_2 agreeing with Case IV, Fig. 7.4.6 in [Guckenheimer & Holmes, 1986], but with the sign of μ_2 flipped. All of these two-dimensional phase portraits for the case $k = +1$ are shown in Fig. 9 of Sec. 3.3.5.

3.3.2. Neighborhoods of HC_1 , HC_2 and TC

Now consider the dynamics near points HC_1 and HC_2 in Fig. 6, for which the coordinates in parameter space are given by Eqs. (56), (57). The corresponding coordinates of the four equilibrium points in the 2D state space are

$$\begin{aligned}
 HC_1 : \quad r &= 0, \quad z_1 = z_4 = 2\sqrt{\frac{\mu_3}{3}}, \\
 z_2 &= z_3 = -\sqrt{\frac{\mu_3}{3}}, \\
 HC_2 : \quad r &= 0, \quad z_1 = z_4 = -2\sqrt{\frac{\mu_3}{3}}, \\
 z_2 &= z_3 = \sqrt{\frac{\mu_3}{3}}.
 \end{aligned} \quad (63)$$

It is clear that HC_1 and HC_2 represent transverse intersections of the bifurcation varieties C and H . From Eq. (63) at each of HC_1 and HC_2 the equilibria E_1 and E_4 have coalesced, corresponding to the Hopf bifurcation on H . Simultaneously E_2 and E_3 have coalesced, corresponding to a fold bifurcation on C . For fixed $\mu_3 > 0$, Eq. (63) shows that in each case these two degenerate equilibria are well-separated in state space. A local bifurcation analysis at each equilibrium involves only classical codimension-one pitchfork and fold bifurcations, respectively, with no interactions between them. Thus, we say these are *trivial codimension-two* bifurcations. The corresponding phase portraits are easily obtained by classical methods and are presented in Sec. 3.3.5. For more details of these calculations, see [Harlim, 2001].

The situation at TC in Fig. 6(b) is similar. There is a secondary Hopf bifurcation at E_4 (with $r > 0$) along T . According to Proposition 2.2 this Hopf bifurcation is supercritical to the right of TC in Fig. 6(b). Independently, a fold bifurcation involving E_3 and E_4 occurs on crossing C . These two codimension-one bifurcations do not interact and the equilibrium E_1 remains hyperbolic near TC . This is another trivial codimension-two bifurcation. However, HtC in Fig. 6(b) is nontrivial and is analyzed in the next section.

3.3.3. Phase plane analysis

At the codimension-two points ZH_1, ZH_2, \dots, HtC in Fig. 6, we have nonlocal behavior in the phase plane. In each case, we need to combine the local results from the codimension-one and two bifurcations, to obtain “global” phase portraits of Eq. (25). Here by “global” we only mean a description of the dynamics in a full neighborhood in which the normal form (25) gives a valid description. Nullclines and the Poincaré–Bendixson Theorem are useful tools to achieve this goal. The nullclines of (25) are

$$\begin{aligned} \dot{r} = 0 &\Rightarrow z = -\mu_1 \quad \text{or} \quad r = 0, \\ \dot{z} = 0 &\Rightarrow r^2 = k[z^3 - \mu_2 - \mu_3 z] \geq 0. \end{aligned} \quad (64)$$

The first two nullclines are straight lines, but the $\dot{z} = 0$ nullcline is nonlinear (S-shaped) and is defined only for $r^2 \geq 0$; see Fig. 7 for the case $k = -1$.

The intersections of the S-shaped nullcline with the z -axis ($r = 0$) give one to three equilibria: E_1 , E_2 and E_3 . Intersection with the horizontal line $z = -\mu_1$ (not shown but easily visualized in Fig. 7)

when $r > 0$ yields E_4 . In the $r > 0$ half-plane, the direction field points to the left below $z = -\mu_1$, and to the right above $z = -\mu_1$. For the S-shaped nullcline $\dot{z} = 0$, if $k = -1$, the direction field points upward in any region on the left side of this nullcline and downward on the right side. The case $k = +1$ can be completed by similar arguments. The following Proposition is a useful tool.

Proposition 3.2. *Consider Eq. (25) with parameters fixed to be in any one of the regions **6a**, **6b**, **6c** of Fig. 6(b). Then there exists a periodic orbit bounded by the unstable manifold of the saddle-point equilibrium E_1 . Moreover, the unstable focus E_4 is in the interior of this periodic orbit.*

Proof. The regions **6a**, **6b**, **6c** of Fig. 6(b) correspond to region **2** in Fig. 7 and the nullcline for $\dot{z} = 0$ is the S-shaped curve in subfigure **2**. The horizontal nullcline $z = -\mu_1$, denoted N_1 in Fig. 8, intersects the S-shaped nullcline at E_4 (between the two turning points because it is interior to the variety T). Any solution orbit meeting N_1 crosses vertically upward between E_4 and the z -axis, and vertically downward on the other side of E_4 . Let $W^U(E_1)$ be the unstable manifold of E_1 . The direction field implies that $W^U(E_1)$ must cross N_1 downward to the right of E_4 , after which $W^U(E_1)$ crosses the S-shaped nullcline below N_1 and eventually meets N_1 to the left of E_4 at s , see Fig. 8. Let K_2 be the “big snail” closed curve, consisting of the segment of $W^U(E_1)$ from E_1 to s , then N_1 to u on the z -axis and finally back to E_1 . Similarly, since E_4 is an unstable spiral point from Sec. 2.2, there exists a “small snail” closed curve K_1 . Finally, consider the closed annular region K bounded by K_1 and K_2 in Fig. 8. Since K is compact, positively invariant, and has no equilibrium points, by the Poincaré–Bendixson Theorem there exists a periodic orbit in K . ■

Proposition 3.2 guarantees existence of a periodic orbit throughout regions **6a**, **6b**, **6c** of Fig. 6(b), but does not guarantee uniqueness. However, with the uniqueness result of Proposition 3.1 of Sec. 3.2, there is a unique and stable limit cycle locally in the interior of regions **6a**, **6b**, **6c** for sufficiently small $\mu_3 > 0$, and this limit cycle is “born” in Hopf bifurcations on crossing the boundaries T of regions **6a**, **6c** in Fig. 6. Uniqueness of the limit cycle also follows in region **4** (see Fig. 10), sufficiently near ZH_1 , from the fold–Hopf theory.

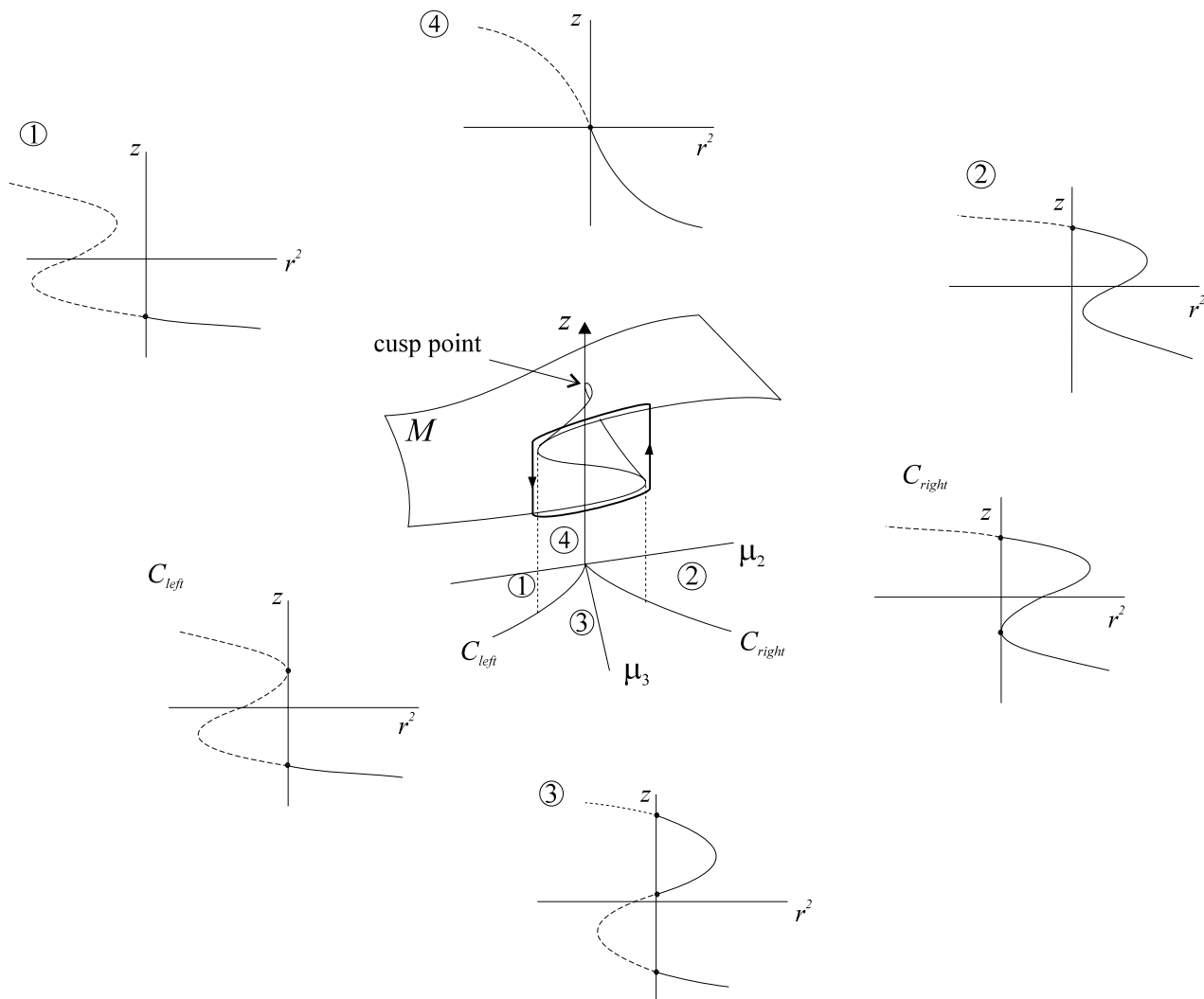


Fig. 7. Dependence of the S-shaped nullcline $\dot{z} = 0$ on the parameters (μ_2, μ_3) , in the case $k = -1$. Only $r^2 > 0$, here drawn with a solid line, is relevant.

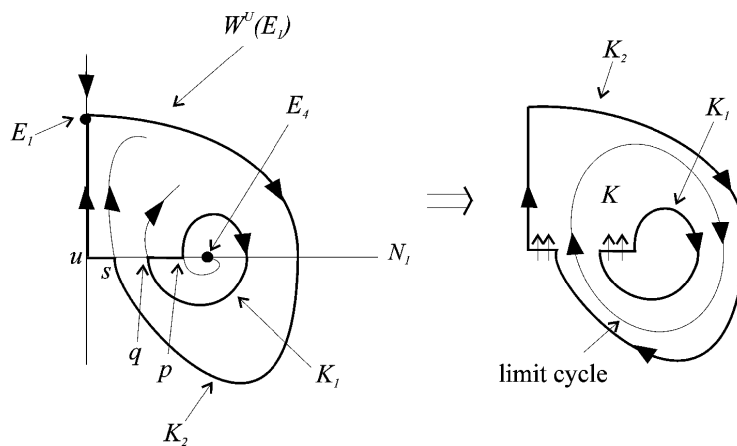


Fig. 8. Illustration of the proof of Proposition 3.2.

Uniqueness on C_3^+ has not been proven, but it is reasonable to assume it holds there too.

We now return to the issue of persistence of the bifurcation varieties Ht and J above C_1^+ , see Fig. 6(b). These were “inherited” from the fold–Hopf bifurcations at ZH_1 and ZH_2 , respectively. Recall that Ht is a heteroclinic loop bifurcation variety, in which the stable and unstable manifolds of two saddle points on the z -axis coalesce to form a closed loop together with the portion of the z -axis joining them. Note that above C_1^+ there exists only one saddle point; the second one disappeared with a node in a fold bifurcation on crossing C_1^+ . Therefore, Ht cannot exist above C_1^+ and Ht globally disappears on crossing C_1^+ through HtC . Below C^+ , Ht persists to account for the disappearance of the limit cycle from region 4 to region 5; see Fig. 10.

At HtC , Ht meets C^+ tangentially rather than transversally, as indicated in Fig. 2 of [Gavrilov, 1987]. Let (μ_1^c, μ_2^c) and (r_2^c, z_2^c) be the parameter values and corresponding coordinates at HtC , where $\mu_2^c = 2[\mu_3/3]^{3/2}$, $r_2^c \equiv 0$ and $z_2^c = -(\mu_2^c/2)$. Write $\Delta z_2 = z_2 - z_2^c$, $\Delta \mu_1 = \mu_1 - \mu_1^c$ and $\Delta \mu_2 = \mu_2 - \mu_2^c$. In a neighborhood of the saddlenode bifurcation, generically

$$\Delta z_2 \propto [-\Delta \mu_2]^{1/2}. \quad (65)$$

As the parameters move toward HtC along Ht , in order for the heteroclinic loop always to meet z_2 which is moving downward according to (65), the loop must grow larger. From (25), the loop grows with increasing μ_1 and generically to leading order this growth will be linear, thus

$$\Delta z_2 \propto -\Delta \mu_1. \quad (66)$$

Combining (65) and (66) gives the approach to HtC along Ht

$$-\Delta \mu_1 \propto [-\Delta \mu_2]^{1/2} \quad \text{as} \quad \Delta z_2 \rightarrow 0, \quad (67)$$

from which follows that Ht is tangent to C^+ at HtC .

At the codimension-two point HtC the heteroclinic loop is degenerate, since the lower saddle point has become a saddlenode. The phase portrait at HtC has a loop, like the heteroclinic loop of case Ht in Fig. 10, except that it tends to the saddlenode along the boundary of its stable set. All orbits inside the loop spiral outward towards the loop. All orbits outside of the loop are attracted eventually to the saddlenode from below as in subfigure C_1^+ of Fig. 10.

Similarly at ZH_2 , J corresponds to the “blow-up” of the periodic orbit created by a Hopf bifurcation in the fold–Hopf case. The phase plane analysis of the cusp–Hopf normal form (25) and Propositions 3.2 and 3.1 show that in this region of parameter space, the periodic orbit persists, is unique and remains finite in a neighborhood of E_4 . Thus, J does not exist in the cusp–Hopf case, and regions **6a**, **6b**, **6c** above C^+ in Fig. 6 are all topologically equivalent for sufficiently small $\mu_3 > 0$. Hereafter they are all labeled **6**.

3.3.4. Fold–heteroclinic bifurcation

An interesting phenomenon occurs on crossing C_1^+ from region **5** to region **6**. A bifurcation occurs that is quite similar to the well known *fold–homoclinic bifurcation*, see [Kuznetsov, 2004]. The heteroclinic case differs from the fold–homoclinic bifurcation in that there exist two saddle points in the loop. A limit cycle is created on crossing C_1^+ , as has been noted in [Gavrilov, 1987; Langford, 1983, 1984b].

In region **5** all but one of the trajectories leaving the unstable focus E_4 go to the stable node on the lower z -axis, so there can be no periodic orbit in region **5** (see subfigure **5** in Fig. 10). The saddle point and nodal sink that exist on the lower, z -axis in region **5** come together in a saddlenode point on C_1^+ (as seen in subfigure C_1^+ in Fig. 10) and then vanish on entering region **6**. The orbits that had gone to the sink now continue upward along the z -axis and around the periodic orbit (the existence of which is guaranteed by Proposition 3.2) in region **6** of Fig. 10. In fact, these orbits must asymptotically approach the periodic orbit, as follows from the uniqueness result of Proposition 3.1 and the Poincaré–Bendixson Theorem. The same is true for those orbits inside the periodic orbit. Thus, an asymptotically stable *limit cycle* is created on crossing C_1^+ . This phenomenon is called a *fold–heteroclinic bifurcation*. The fold–heteroclinic bifurcation leads to interesting behavior in the three-dimensional dynamics that we call *bursting oscillations*, see Sec. 4.

3.3.5. 2D bifurcation diagrams and phase portraits

This section completes the presentation of bifurcation diagrams and planar phase portraits. For the simpler case of $\mu_3 < 0$ the results are shown already in Fig. 4. Here we complete the case $\mu_3 > 0$.

Without loss of generality, fix $l = -1$, $m = +1$, and consider both cases $k = \pm 1$.

The case $k = +1$ is shown in Fig. 9. On crossing either of the two horizontal lines C^+ or C^- from the region between them, two equilibrium points on the z -axis coalesce and vanish via a fold bifurcation. The S-shaped curve H locates the pitchfork bifurcation in the two-dimensional system and corresponds to the primary Hopf bifurcation in the three-dimensional system. Everywhere to the left and below H there exists a saddle point E_4 with $r > 0$, and there are two to four equilibria. Above H , the equilibrium E_4 does not exist and there are at most three equilibria. There are no limit cycles.

Now consider the more interesting case $k = -1$, see Fig. 10. In addition to the bifurcations on C and H as above, there is a secondary Hopf (Torus) bifurcation on crossing T , a heteroclinic loop bifurcation in which a limit cycle disappears

on crossing Ht from region 4 to region 5, and a fold-heteroclinic bifurcation that gives rise to a limit cycle on crossing C_1^+ from 5 to 6. Call the part of region 6 along C_1^+ above 5 a *bursting region*.

If μ_3 decreases continuously to 0 and becomes negative, then in Fig. 9 or 10 the cusp variety C^\pm shrinks to the μ_1 -axis and disappears together with many of the phase portraits, leaving only the two portraits 1 and 6 as in Fig. 4(a) ($k = +1$), or the two portraits 1 and 9 as in Fig. 4(b) ($k = -1$), respectively.

Figures 9 and 10 present all of the structurally stable two-dimensional phase portraits, and most of the nonstructurally stable transitional portraits on the bifurcation varieties, for $l = -1$, $m = +1$ and $\mu_3 > 0$. All the remaining of the eight cases $k = \pm 1$, $l = \pm 1$, $m = \pm 1$ may be obtained from the two presented here on applying the transformations (22), (23) of Sec. 2.

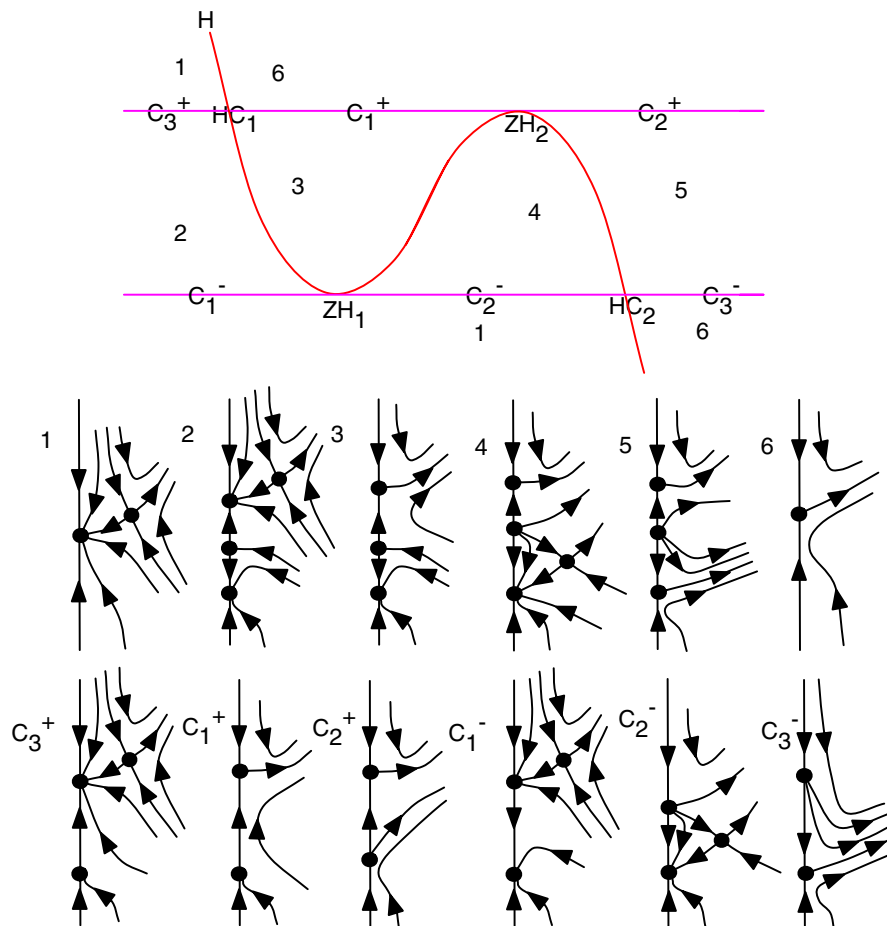


Fig. 9. 2D bifurcation diagram and phase portraits for $k = +1$ (with $l = -1$, $m = +1$, $\mu_3 > 0$).

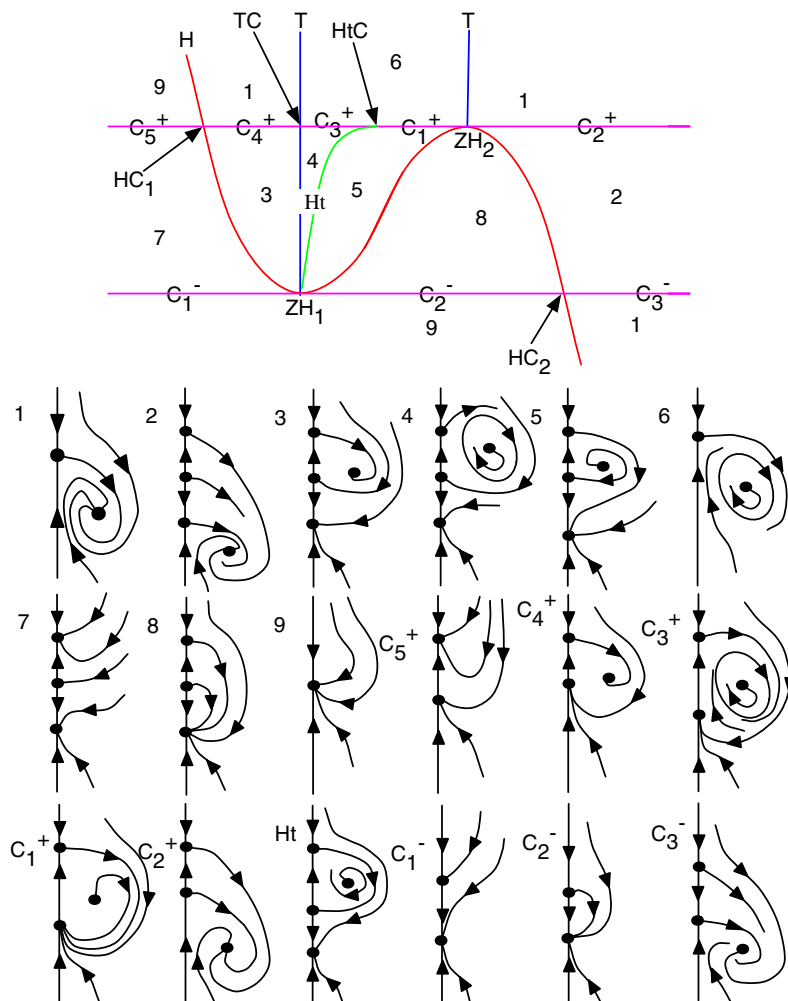


Fig. 10. 2D bifurcation diagram and phase portraits for $k = -1$ (with $l = -1$, $m = +1$, $\mu_3 > 0$).

4. Three-Dimensional Phase Portraits

This section presents selected three-dimensional phase portraits for the cusp–Hopf bifurcation, emphasizing behavior that is not typical of the fold–Hopf case, and indicates where the study of the 3D dynamics is incomplete.

Consider the bifurcation diagrams for the two-dimensional (r, z) system (25), shown in Figs. 4, 9 and 10. To this (r, z) system, now restore the θ dependence, but first in the restricted form of the truncated Eqs. (11), (12). This three-dimensional system has an S^1 symmetry of rotation around the z -axis. Note this is not a rigid rotation, but rather rotation with “shear”, that is, the angular velocity can be different on each circle $O_{r,z}$ through (r, z) with center at $(0, z)$. Locally, the rate of rotation about the z -axis is asymptotically close to ω . With these observations, the phase portrait of the truncated three-dimensional system is obtained easily

by rotation of the two-dimensional phase portraits in Sec. 3.3.5 about the z -axis, taking into account the shear.

The trivial equilibria $E_{1,2,3}$ remain equilibrium points on the z -axis for the truncated three-dimensional system (11), (12) and the surface C remains a fold bifurcation surface for these equilibria. The nontrivial equilibrium E_4 with $r \neq 0$ in (25) corresponds to a periodic orbit in (11), (12), with the same stability as E_4 . This periodic orbit is created in a Hopf bifurcation on H . The secondary Hopf bifurcation surface T corresponds to a Neimark–Sacker bifurcation of the limit cycle in (11), (12), giving rise to an invariant two-torus. This torus is the same torus that exists in the fold–Hopf bifurcations at $W1$ and $W2$ if $k = -1$. The heteroclinic loop that exists on Ht in the planar system is rotated about the z -axis to generate a smooth two-dimensional invariant surface for (11), (12).

Next, consider the effects of restoring the higher order terms to (11), (12), as in (10). These higher order terms break the S^1 symmetry. This may dramatically affect the dynamics. Still, much of the behavior of the S^1 -symmetric system does persist. The key property is “normal hyperbolicity”. Orbits or invariant manifolds which are hyperbolic in directions normal to the flow direction (essentially the direction of the S^1 symmetric rotation) are structurally stable and therefore preserved under sufficiently small perturbations; even those that break the S^1 symmetry. Solutions of the two-dimensional system that are hyperbolic in the (r, z) phase plane become normally hyperbolic solutions in the three-dimensional space. Thus hyperbolic equilibria and limit cycles persist. The asymptotically stable limit cycle in the (r, z) phase plane becomes a normally hyperbolic invariant torus that persists, at least locally.

The three-dimensional solutions of the S^1 -symmetric normal form Eqs. (11) and (12) are represented in figures obtained numerically using MAPLE. These simulations confirm the above predictions regarding the system with S^1 symmetry. Combining the planar Eq. (25) with a rigid rotation $\dot{\theta} = \omega$ and transforming back to cartesian coordinates gives

$$\begin{aligned}\dot{x} &= (z + \mu_1)x - \omega y \\ \dot{y} &= \omega x + (z + \mu_1)y \\ \dot{z} &= \mu_2 + \mu_3 z - z^3 + k(x^2 + y^2).\end{aligned}\quad (68)$$

In region **1** of Fig. 10, the flow converges to a limit cycle about the z -axis, as can be seen in Fig. 11(a) corresponding to parameters $\mu_3 = 1$, $k = -1$, $\mu_1 = -0.6$, $\mu_2 = 0.4$, $\omega = 3.5$ and initial condition $x(0) = 0.1$, $y(0) = 0.1$, $z(0) = 0.1$. Now cross

T to region **6**, choose $\mu_1 = -0.5$ but keep the other values as in Fig. 11(a). Then a torus is observed as in Fig. 11(b).

In region **4** of Fig. 10, choose parameters $\mu_3 = 1$, $k = -1$, $\mu_1 = -0.55$, $\mu_2 = 0$ and $\omega = 3.5$, and solve (68) numerically with two sets of initial conditions, namely $x(0) = 0.1$, $y(0) = 0.1$, $z(0) = 1$, and $x(0) = 0.1$, $y(0) = 0.1$, $z(0) = -0.1$. In this case *bistability* is observed: the first initial point leads to an invariant torus, while in the second case the flow converges to the stable node. This is consistent with the two-dimensional dynamics in region **4** of Fig. 10. The three-dimensional phase portraits are in Fig. 12.

The nature of the flow on the invariant torus is influenced as follows by the higher order remainder terms. The S^1 symmetry of the truncated system (11), (12) implies that all of the orbits in the invariant torus are S^1 -conjugates. This means that, given any orbit γ in the invariant torus and any group element $\sigma \in S^1$, then $\sigma\gamma$ is always an orbit in the invariant torus, and furthermore every orbit on the torus is obtained in this way. When the S^1 symmetry is broken, the orbits are no longer constrained in this way and the nature of the flow is determined by a rotation number ρ , see Sec. 6.2 in [Guckenheimer & Holmes, 1986]. The rotation number ρ in the present case is essentially the ratio of the two frequencies of the secondary and the primary Hopf bifurcations, that is $\sqrt{\mu_2 - 2\mu_1^3}/\omega$; therefore, ρ is a very small number. If ρ is an irrational number, then there is a nonperiodic dense orbit in the invariant torus. If ρ is a rational number, then generically there are interlaced stable and unstable periodic orbits on the invariant torus, which have very long period since ρ is small; one calls this is “weak resonance”. Because ρ is small, this

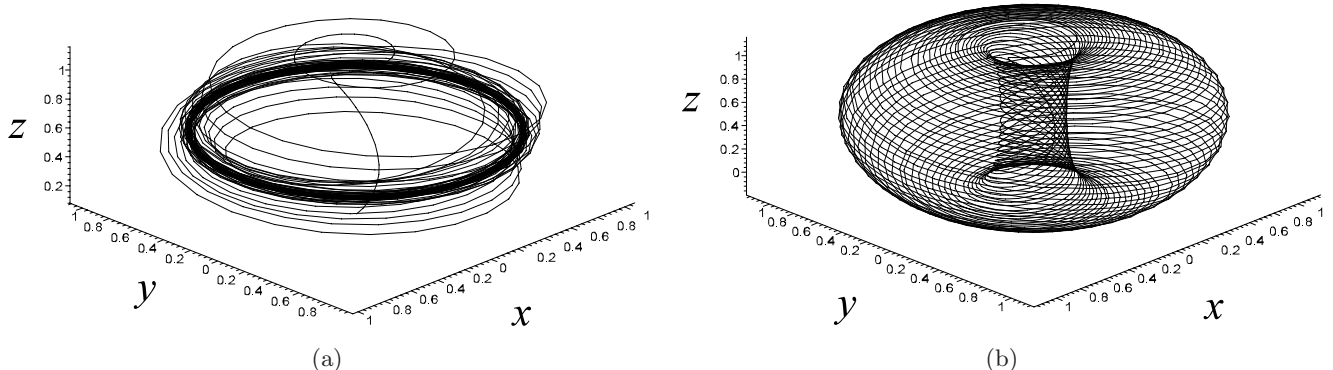


Fig. 11. Example of bifurcation from a stable limit cycle to an invariant torus. (a) Stable limit cycle in region **1**. (b) Symmetric torus attractor in region **6**.

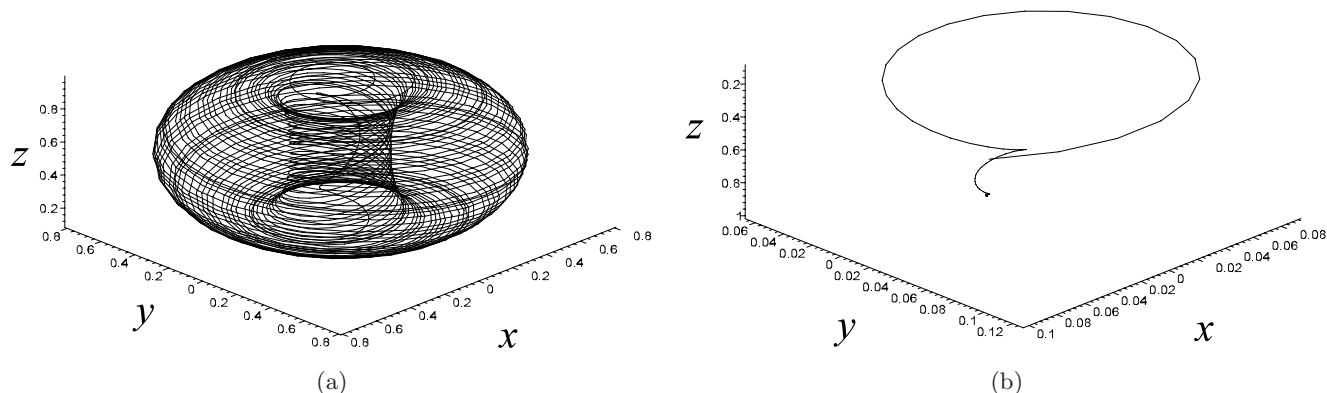


Fig. 12. Example of bistability in region 4 of Fig. 10. (a) Torus attractor. (b) Equilibrium point attractor. For initial conditions, see text.

distinction between the irrational case (nonperiodic orbits) and the rational case (very long periodic orbits) is only academic; in practice, they cannot be distinguished without very careful measurements or computations.

There is another more significant effect that S^1 symmetry-breaking may have on the invariant torus. It may cause the torus to lose smoothness and “wrinkle”, even under fairly small symmetry-breaking perturbations, sufficiently near the heteroclinic loop Ht . An early numerical study of the cusp-Hopf bifurcation, Langford [1984b], showed that, near the former invariant torus of the symmetric equations, one can find not only periodic orbits, but also period doubling, coexistence of attractors and a variety of chaotic attractors, including a “Cantor band” and a “thickened wrinkled torus”. The origin of much of this chaotic behavior is the heteroclinic loop in the (r, z) half-plane, that exists on Ht , which generates a two-dimensional sphere-like invariant manifold for the S^1 -symmetric system (11), (12). This surface in general splits into two 2-manifolds, respectively the stable and unstable manifolds of the two saddle points, and these manifolds generically intersect transversely but infinitely often, giving rise to Smale horseshoes and related generic chaotic phenomena that have been studied by many people since Poincaré. Another effect of the S^1 symmetry-breaking perturbations is the fact that the z -axis need no longer be invariant, so the three equilibria $E_{1,2,3}$ are no longer joined by unique heteroclinic orbits along the z -axis. Instead, these one-dimensional stable and unstable manifolds are freed to escape the z -axis and may find their way to strange (Silnikov) attractors. These chaotic phenomena are not pursued further in this paper.

4.1. *Bursting oscillations*

A system is said to have bursting oscillations when its activity changes periodically between a quiescent state and a train of rapid spike-like oscillations. Hysteresis or bistability of a fast subsystem is a typical ingredient of systems exhibiting bursting activity. Such systems are often studied using perturbation theory with two timescales (fast and slow) with the convention that the slow system parametrizes the fast system. Schemes for the classification of bursters have been proposed by various authors, see for example [Rinzel, 1987; Izhikevich, 2000].

Just after the saddle point and node on the z -axis disappear in a saddlenode bifurcation on C_1^+ in Fig. 10, the vector field remains *nearly zero* in a neighborhood that formerly contained the saddlenode point. This implies that the flow of solutions through this neighborhood is very slow. Thus, on the newly-created limit cycle the flow is very slow near this part of the z -axis where the saddle-node had been, and relatively fast on the portion away from the z -axis. On restoring the θ dependence, the three-dimensional system (11), (12) has solutions that oscillate with relatively large amplitude r and fast frequency, then decay to very small amplitude and appear quiescent near the z -axis for an interval of time, after which they rebound to large fast oscillations again. Numerical examples of such bursting oscillations have been given in Langford [1983, 1984b].

Numerical simulation for the three-dimensional system (68), with parameters corresponding to region 6 of Fig. 10 near the fold-heteroclinic bifurcation, yields a bursting oscillation. See Fig. 13(a) for a partial phase portrait. Figure 13(b) shows the plot of x versus time t for the same solution, which confirms bursting activity for Eq. (68) in region 6 near

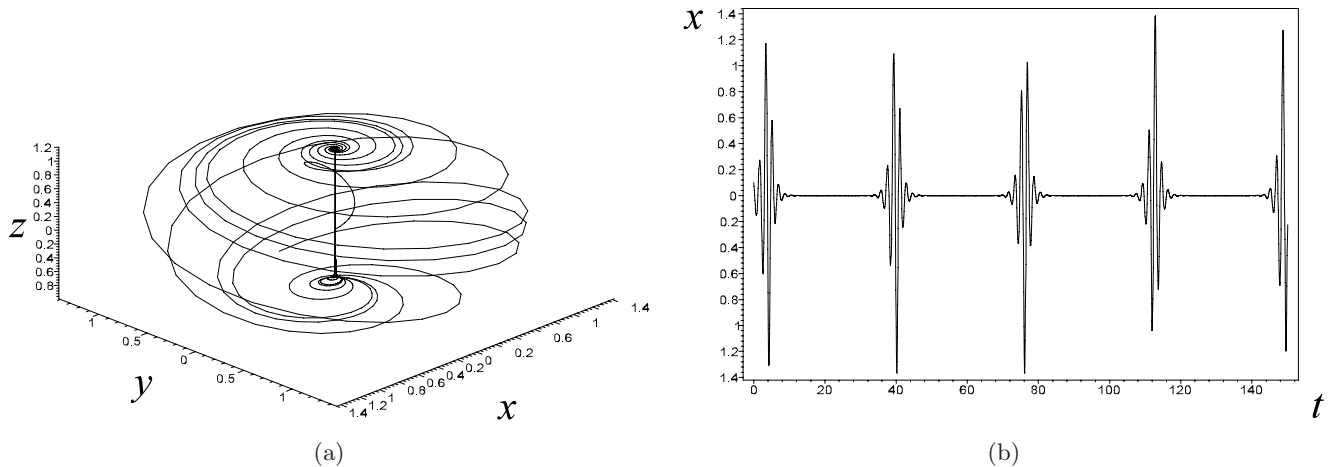


Fig. 13. (a) Bursting oscillations in three-dimensional state space, parameter region **6** near **5** in Fig. 10. (b) Graph of $x(t)$ with respect to time t .

C_1^+ . Both plots were calculated with initial condition $x(0) = 0.1$, $y(0) = 0.1$, $z(0) = 0.1$, and parameters $k = -1$, $\mu_1 = -0.2$, $\mu_2 = 0.4$, $\mu_3 = 1$.

5. Conclusions and Future Directions

The generalization of the classical codimension-two fold–Hopf bifurcation, to a codimension-three cusp–Hopf bifurcation, yields a variety of new and interesting phenomena. In this paper, analysis of the cusp–Hopf system with three bifurcation parameters leads to the stratified subvariety of primary bifurcations presented in Fig. 3. Nonlinear term coefficients k , l and m contribute eight different cases to the analysis, but these have been reduced to two cases by rescalings including time reversal.

The unfoldings of the cusp–Hopf bifurcation incorporate all four generic cases of the codimension-two fold–Hopf normal form. This, together with classical nullcline analysis and the degenerate Hopf bifurcation theorem of [Golubitsky & Langford, 1981], guides us to understanding all of the possible behaviors of the truncated cusp–Hopf system in the two-dimensional (r, z) coordinates, as displayed in Figs. 4, 9 and 10. An important property for applications is that, in the case $k = -1$, the cusp–Hopf bifurcation has a basin of attraction. This is impossible for the fold–Hopf bifurcation.

Also, in the three-dimensional dynamics for $k = -1$, a torus may exist in the truncated normal form arising via a Neimark–Sacker bifurcation from a limit cycle. It may be expected to persist for parameter values near this bifurcation. Further

away, near a heteroclinic loop, the symmetry-breaking remainder terms cause the torus to lose its smoothness and it may be replaced by a chaotic attractor. Further investigation of such chaotic behavior and the occurrence of Melnikov and Silnikov phenomena will be reported elsewhere.

A *fold-heteroclinic bifurcation* gives rise to a limit cycle, via a fold bifurcation in a heteroclinic cycle connecting a saddle point and a saddlenode point. This bifurcation does not occur in the fold–Hopf case. It plays an important role in the occurrence of “bursting oscillations” in the three-dimensional dynamics. Numerical simulations confirm the bursting oscillations.

Finally, we propose that neural network models as in [Izhikevich, 2000; Rinzel, 1987] and physical systems as in [Mullin, 1993; Roux, 1985] will be investigated to determine whether the type of bursting behavior identified here, in a codimension-three normal form, may be relevant to the understanding of bursting behavior in such applications.

Acknowledgments

The authors would like to thank J. Holbrook and H. Kunze for their constructive criticism of [Harlim, 2001] and D. D. Rusu and H. Sendov for providing translations of the papers of Gavrilov [1987]; Gavrilov and Roschin [1983] respectively, from Russian into English. They also thank A. Willms for constructing region R in the proof of Proposition 2.1 and an anonymous referee for indicating that Ht approaches C^+ tangentially at HtC , as in [Gavrilov, 1987].

References

- Algaba, A., Freire, E. & Gamero, E. [1998] "Hypernormal form for the Hopf-zero bifurcation," *Int. J. Bifurcation and Chaos* **8**, 1857–1887.
- Chow, S.-N., Li, C. & Wang, D. [1994] *Normal Forms and Bifurcation of Planar Vector Fields* (Cambridge University Press, Cambridge).
- Dangelmayr, G. & Armbruster, D. [1983] "Classification of $\mathbb{Z}(2)$ -equivariant imperfect bifurcations with corank 2," *Proc. London Math. Soc.* **46**, 517–546.
- Freire, E., Gamero, E., Rodriguez-Luis, A. J. & Algaba, A. [2002] "A note on the triple-zero linear degeneracy: Normal forms, dynamical and bifurcation behaviors of an unfolding," *Int. J. Bifurcation and Chaos*, **12** 2799–2820.
- Gavrilov, N. K. [1978] "On some bifurcations of an equilibrium with one zero and a pair of pure imaginary roots," *Methods of the Qualitative Theory of Differential Equations* (Gorkii State University, Gorkii, USSR), pp. 33–40 (in Russian).
- Gavrilov, N. K. & Roschin, N. V. [1983] "On stability of an equilibrium state with one zero and a pair of purely imaginary eigenvalues," *Methods of the Qualitative Theory of Differential Equations* (Gorkii State University, Gorkii, USSR), pp. 41–49 (in Russian).
- Gavrilov, N. K. [1987] "Bifurcations of an equilibrium state with one zero root and a pair of purely imaginary roots and additional degeneration," *Methods of the Qualitative Theory of Differential Equations*, ed. Leontovich-Andronova, E. A. (Gorkii State University, Gorkii, USSR), pp. 43–51 (in Russian).
- Golubitsky, M. & Langford, W. F. [1981] "Classification and unfoldings of degenerate Hopf bifurcations," *J. Diff. Eqs.* **41**, 375–415.
- Golubitsky, M. & Schaeffer, D. G. [1985] *Singularities and Groups in Bifurcation Theory, Volume I*, Applied Mathematical Sciences, Vol. 51 (Springer-Verlag, NY).
- Govaerts, W., Guckenheimer, J. & Khibnik, A. [1997] "Defining functions for multiple Hopf bifurcations," *SIAM J. Num. Anal.* **34**, 1269–1288.
- Guckenheimer, J. [1980] "On a codimension two bifurcation," in eds. Rand, D. & Young, L., *Dynamical Systems and Turbulence*, Lecture Notes in Mathematics, Vol. 898 (Springer-Verlag, NY), pp. 99–142.
- Guckenheimer, J. & Holmes, P. [1986] *Nonlinear Oscillations, Dynamical Systems, and Bifurcations of Vector Fields*, Applied Mathematical Sciences, Vol. 70 (Springer-Verlag, NY), Corrected second printing.
- Harlim, J. [2001] "Codimension three Hopf and cusp bifurcations," Master's thesis, University of Guelph.
- Holmes, P. [1980] "Unfolding a degenerate nonlinear oscillator: A codimension two bifurcation," in *Nonlinear Dynamics*, ed. Helleman, R. G. H., Ann. N. Y. Acad. Sci., Vol. 357, pp. 473–488.
- Iooss, G. & Langford, W. F. [1980] "Conjectures on the routes to turbulence via bifurcations," in *Nonlinear Dynamics*, ed. Helleman, R. G. H., Ann. N. Y. Acad. Sci., Vol. 357, pp. 489–505.
- Iooss, G. & Adelmeyer, M. [1992] *Topics in Bifurcation Theory and Applications*, Advanced Series in Nonlinear Dynamics, Vol. 3 (World Scientific, Singapore).
- Izhikevich, E. [2000] "Neural excitability, spiking, and bursting," *Int. J. Bifurcation and Chaos* **10**, 1171–1266.
- Krauskopf, B. & Rousseau, C. [1997] "Codimension-three unfoldings of reflectionally symmetric planar vector fields," *Nonlinearity* **10**, 1115–1150.
- Kuznetsov, Yu. [2004] *Elements of Applied Bifurcation Theory*, Applied Mathematical Sciences, Vol. 112 (Springer-Verlag, NY), 3rd edition.
- Kuznetsov, Yu. [2005] "Practical computation of normal forms on center manifolds at degenerate Bogdanov-Takens bifurcations," *Int. J. Bifurcation and Chaos* **15**, 3535–3546.
- Langford, W. F. [1979] "Periodic and steady-state mode interactions lead to tori," *SIAM J. Appl. Math.* **37**, 649–686.
- Langford, W. F. [1982] "Chaotic dynamics in the unfoldings of degenerate bifurcations," in *Proc. Int. Symp. Applied Mathematics and Information Science* (Kyoto University, Japan), pp. 2.41–2.47.
- Langford, W. F. [1983] "A review of interactions of Hopf and steady-state bifurcations," in *Nonlinear Dynamics and Turbulence*, eds. Barenblatt, G. I., Iooss, G. & Joseph, D. D. (Pitman Advanced Publishing Program), pp. 215–237.
- Langford, W. F. [1984a] "Hopf bifurcation at a hysteresis point," in *Differential Equations: Qualitative Theory*, Colloq. Math. Soc. János Bolyai, Vol. 47 (North Holland), pp. 649–686.
- Langford, W. F. [1984b] "Numerical studies of torus bifurcations," in *Numerical Methods for Bifurcation Problems*, eds. Küpper, T., Mittelman, H. D. & Weber, H., ISNM, Vol. 70 (Birkhäuser Verlag, Basel), pp. 285–295.
- Langford, W. F. & Zhan, K. [1999] "Interactions of Andronov-Hopf and Bogdanov-Takens bifurcations," *Fields Institute Communications*, Vol. 24 (Amer. Math. Soc.), pp. 365–383.
- LeBlanc, V. G. & Langford, W. F. [1996] "Classification and unfoldings of 1 : 2 resonant Hopf bifurcation," *Arch. Rat. Mech. Anal.* **136**, 649–686.
- Mullin, T. [1993] *The Nature of Chaos* (Clarendon Press, Oxford), Chaps. 3 and 4.
- Rinzel, J. [1987] "A formal classification of bursting mechanisms in excitable systems," in *Mathematical Topics in Population Biology, Morphogenesis and Neurosciences*, Lecture Notes in Biomathematics, Vol. 71 (Springer-Verlag, NY), pp. 267–281.

- Roux, J. C. [1985] "Chaos in experimental systems: Two examples," in *Singularities and Dynamical Systems*, ed. Pnevmatikos, S. N. (Elsevier Science Publ.), pp. 345–352.
- Sieber, J. & Krauskopf, B. [2004] "Bifurcation analysis of an inverted pendulum with delayed feedback control near a triple-zero eigenvalue singularity," *Nonlinearity* **17**, 85–103.
- Thom, R. [1975] *Structural Stability and Morphogenesis* (W. A. Benjamin, Reading, MA).
- van Gils, S. A. [1985] "A note on abelian integrals and bifurcation theory," *J. Diff. Eqs.* **59**, 437–441.
- van Gils, S. A., Krupa, M. & Langford, W. F. [1990] "Hopf bifurcation with non-semisimple 1:1 resonance," *Nonlinearity* **3**, 825–850.
- Vanderbauwhede, A. [1986] "Hopf bifurcations with non-simple eigenvalues," in *Multiparameter Bifurcation Theory*, eds. Golubitsky, M. & Guckenheimer, J., *Contemp. Math.*, Vol. 56, pp. 343–353.
- Wiggins, S. [1990] *Introduction to Applied Nonlinear Dynamical Systems and Chaos*, *Texts in Applied Mathematics*, Vol. 2 (Springer-Verlag, NY).
- Zoladek, H. [1987] "Bifurcations of certain family of planar vector fields tangent to axes," *J. Diff. Eqs.* **67**, 1–55.